„DUNĂREA DE JOS” UNIVERSITY OF GALAȚI
Doctoral School of Mechanical and Industrial Engineering

PhD THESIS

-Summary-

Studies regarding chemical and electrochemical nanostructuration of polymers and effects of nanostructuration on mechanical properties of polymers

Chairman	Prof. univ. dr. eng. Mihaela BUCIUMEANU
PhD Supervisor	Prof. univ. dr. eng. Iulian-Gabriel BÎRSAN
Scientific Committee	Prof. univ. dr. eng. Dan-Mihai CONSTANTINESCU Prof. univ. dr. eng. Horia IOVU Prof. univ. dr. phys. Adrian CÎRCIUMARU

Series I6: Mechanical Engineering No. 57
Galați 2021

Programul Operațional Capital Uman
Axa prioritară 6 - Educație și competențe
Proiect: Burse pentru educația antreprenorială în rândul doctoranzilor și cercetătorilor postdoctorat (BeAntreprenor!)
Cod MySMIS: 124539

Studies regarding chemical and electrochemical nanostructuration of polymers and effects of nanostructuration on mechanical properties of polymers

PhD candidate: Mihaela-Claudia GOROVEI

PhD Supervisor: Iulian Gabriel BÎRSAN

The present research is carried out with support of the project

"Scholarships for entrepreneurial education among doctoral students and postdoctoral researchers (Be Entrepreneur!)", Contract no. 51680/09.07.2019 - SMIS code: 124539.

Seriile tezelor de doctorat susținute public în UDJG începând cu 1 octombrie 2013 sunt:

Domeniul **ȘTIINȚE INGINEREȘTI**

- Seria I 1**: Biotehnologii**
- Seria I 2**: Calculatoare și tehnologia informației**
- Seria I 3**. Inginerie electrică**
- Seria I 4**: Inginerie industrială**
- Seria I 5: **Ingineria materialelor**
- Seria I 6**: Inginerie mecanică**
- Seria I 7**: Ingineria produselor alimentare**
- Seria I 8**: Ingineria sistemelor**

Domeniul **ȘTIINȚE ECONOMICE**

- Seria E 1**: Economie**
- Seria E 2**: Management**

Domeniul **ȘTIINȚE UMANISTE**

- Seria U 1**: Filologie- Engleză**
- Seria U 2**: Filologie- Română**
- Seria U 3: **Istorie**

Table of contents

Introduction

Research on composite materials has evolved rapidly and gained popularity due to their higher durability properties. Composites are macroscopic modifications between two or more materials with different physical or chemical properties, to obtain a more efficient and useful third material. Composites are generally the results of intervention on a material (matrix) by adding two or more other materials to its volume, of chemical and mechanical properties, sometimes aesthetics.

Composites have applicability in different industries: construction (pavements, pipes, floor coverings), aeronautical (blades, turbines, flaps, tailings, engine parts), shipbuilding (decks, masts and covers), transport, equipment and medical devices (bandages, towels, patches, operating room equipment), drug delivery systems, bio-absorbable systems, permanent prosthetic devices including hip implants, artificial lenses, large diameter vascular grafts, catheters. Also, many new applications are being developed as a result of major advances in molecular and cell biology.

The most important field of application for polymeric composites is in the automotive industry. The general application areas of composites in the automotive industry are body panels, seals, wheel covers, wings, gaskets, instrument panel, steering wheel, seat and associated parts, instrument panel leather, decorative parts, sensors, compartments ignition, bumpers, wheels, mirror housings, hatches, flaps, spoilers, safety panels, grilles, seat belts, expansion vessels, centre console, dashboard, door panels, door sills.

The optimization of the general properties and better adaptation of specific properties to well-defined applications is a priority of composite research.

Improving mechanical properties requires a better understanding of the multiple dependencies between molecular structure, morphology, processing methods and the final properties of composite materials. The connection between the structure, morphology and mechanical properties are the micromechanical processes or mechanisms that take place at loading at the microscopic and nanoscopic level: the so-called field of micro- and nano-mechanics. The knowledge of these mechanisms is key to the successful development and improvement of already used composites with better properties.

Polymer composites are those for which the matrix is made of a polymer which includes reinforcing elements, fillers, fillers, additives or other introduced agents to modify one or another of the properties of the polymer.

As is known, polymers are classified into three main categories - thermoplastic polymers, thermosetting polymers and elastomers. Each of these classes is characterized by common properties.

Thermoplastic polymers melt when heated, weakening their intermolecular forces (through the thermal vibrations of molecules) and solidify upon cooling, returning to their initial strength and hardness if certain processing conditions are met.

Thermosetting polymers are permanently hardened due to irreversible chemical reactions (cross-linking). Unlike thermoplastic polymers, the properties of thermosetting polymers are preserved even with the temperature value increasing. Epoxy matrix composites are used in a large number of applications in various industries, including the aerospace, automotive and electronics industries. This wide range of applications is due to the favourable thermomechanical properties of these resins and the ease of their processing.

The main arguments for the use of composites are:
- easy processability, modelability (manufacture of difficult shapes);
- low production costs (better energy balance per volume than many other materials, for example, steel or aluminium);
- advantageous strength / density ratio;
- resistance to many chemicals and moisture (corrosion resistance, environmental stability);
- great diversity of properties (mechanical, optical, electrical, among others);
- the possibilities of modification with organic or inorganic agents;
- recyclability - in the case of all thermoplastic polymers and thermosetting polymers (material or energy recycling).

Epoxy resins are usually obtained by mixing two chemical substances in a liquid state, a mixture that solidifies as a result of chemical reactions between the two components commonly called resin and hardener, respectively. This is not only the case for epoxy resins and not all epoxy resins are obtained in this way. The enormous advantage of using epoxy resins obtained from the chemical reaction between resin and hardener is that it allows intervention on the properties of the final polymer even before mixing the two components, by introducing agents – by solubilising (in the most favourable case) – what could change the properties of the polymer.

At the Research and Development Center for thermosetting composites (CCDCOST) at the cross-border Faculty of the University Dunărea de Jos din Galați, have been carried out in recent years, various studies on the properties of epoxy matrix composites and how these properties can be modified to accumulate data that finally allows the design of the properties of epoxy matrix composite materials and structures. Most studies, at CCDCOT, have been carried out on the Epiphen epoxide system RE4020-DE4020 and for this reason, the present study is taking note of this epoxy resin.

1. Nanostructures and nanostructuration of polymeric matrices

There are certain polymeric systems with unique properties that can be directly attributed to the presence of structural entities with nanometric dimensions. Due to the special contribution of these nano-sized entities, this class of polymeric systems can be designated, as a whole, as nanostructured polymeric materials [1].

Nanostructured polymers and hybrid inorganic-organic nanocomposites have gained popularity in the last two decades due to their special properties, volume or surface. The nanostructuring control of polymers and the addition of nanoparticles have led to improvements in structural and functional properties in several polymeric systems in response to the continuing requirements of advanced industrial sectors. Therefore, most research efforts in this field have focused on developing rational processing strategies for nanostructured polymers and composites and on promoting a better interaction between matrix and nanoparticles [2] - [5].

Nanostructured polymeric materials, including micelles, nanoparticles, nanocapsules, nanogels and nanocomposites, can be prepared in several ways. Their properties, such as stability, size, shape, electrostatic charge of the surface, surface chemistry, mechanical strength, porosity, among others, can be adapted to the specific functionalities that are needed to meet the needs in different applications [6] - [8]. The superior stability of polymeric nanostructures over surfactant-based micelles makes them ideal candidates to protect catalytic functionalities from the external environment for an extended shelf life [9], [10].

1.1. Polymer materials

Polymers are abundant in nature, they are found in all living systems and in various materials such as wood, paper, leather, natural fibres, being widely used. While natural polymers retain their intrinsic importance, currently the synthetic materials are mostly used [11] - [14].

The term *polymer* comes from the Greek words *poly* (many) and *meros* (part). Polymers are made up of a large number of identical small molecules called monomers [15].

Polymers have a wide range of physical and mechanical properties, which are suitable for a large number of technical applications [26]. The main fields of application of polymers are plastics, rubber or elastomers, fibres, surface finishes, coatings and adhesives [27], [28].

The chemical structure, average relative molecular mass and its distribution, chain conformity, morphology, additives and reinforcing fillers are witnesses to define the individual properties of materials and to allow sophisticated adaptation of materials to specific applications [29]. Because most polymers are low-density materials, they have specific advantages in the transportation industry, by replacing metals, medical equipment and devices, drug delivery systems, bio-absorbable systems, permanent prosthetic devices including hip implants, artificial lenses, vascular grafts with large diameter, catheters [30]. Several new applications are also being developed as a result of major advances in molecular and cell biology [17], [31], [32], [33], [34].

1.3. Nanostructured resins

In 1907, Leo Baekeland invented the first synthetic polymer, a phenol-formaldehyde resin called bakelite, which is made from chemically crosslinked polymer chains. As such, it was the first sample of a whole class of polymeric materials: the so-called thermosetting polymers.

Materials with thermosetting resins (epoxy) are used in a large number of applications in various industries, including the aerospace, automotive and electronics industries. This wide range of applications is due to the favourable thermomechanical properties of these resins and the ease of their processing [63] - [69].

From a production point of view, thermoset resins are generally made from a liquid mixture, initially of polyfunctional organic molecules that gradually react with each other to form a three-dimensional solid network, while thermoplastics are marketed as solid pellets and moulded into their final shape by melting [70]. Advantageously, the low molecular weight of the thermoset precursors allows the formation of reactive mixtures with low viscosity which offer unique flexibility in applications, such as coating or wetting of fibres. However, it also requires a fine-grained control of the viscosity kinetics that ultimately comes with a transition from liquid to solid: gelation [71] - [75].

Epoxy resins are among the most widely used types of materials in the industrial field due to their distinct mechanical properties and the fact that they are inexpensive. When formulated correctly, epoxy resins have excellent mechanical strength, chemical resistance, adhesion, relatively high temperature resistance and structural stability. Thus, components made of epoxy resins have great potential for application as functional organic materials in bonding agents, flame retardants in IT devices and structural reinforcement systems [76] - [88].

1.5. Researches on nanostructures and polymers nanostructuration

S. E. Jasim and his collaborators [135] manufactured YBCO superconducting nanoparticles (copper oxide, barium and yttrium) by the electrochemical method of electrospinning. The temperature transition of the YBCO nanoparticle thin film showed a zero resistance at 78K, with a semi-sharp transition width of 13K while the blank material indicated zero resistance at 85K and a sharp transition width of 6K. A typical nanoparticle diameter between 20nm and 50nm was obtained and agglomerations of nanoparticles of about 388nm were achieved. The measured surface area of the YBCO nanoparticle was larger than that of the blank material and was not influenced by the calcination temperature.

Lu et al [137] fabricated PVP/Ag_2S nanoparticles in ethanol solution. The obtained black viscous solution was loaded into a plastic syringe equipped with a 14cm platinum needle. The needle was connected to a high voltage source (15 kV) which was applied to the electrospinner. A piece of flat aluminium foil was placed 20 cm from the tip of the needle to collect the nanofibers. Electrospinning was performed under normal conditions (air). Fibre images were taken using scanning electron microscopy. Ag_2S nanoparticles were characterized by transmission electron microscopy.

Vyacheslav V. and co-workers [138] manufactured composite fibres by the intermediate electrospinning method containing $ZrOCl_2$ and $Al(NO_3)_3$ as ZrO_2 and Al_2O_3 precursors, with PVP as additive. The mean fibre diameter was 284 ± 69nm. The data obtained by EDS indicate that the fibres prepared from the electrospinning solution contain the polymer precursors detected by the presence of the element C, ZrO_2 and Al_2O_3 (Zr, Cl, Al, N). The presence of the two distinct phases was highlighted: ZrO_2 (lighter phase) and Al_2O_3 (dark phase). They noticed that Al_2O_3 is partially dissolved. $ZrOCl_2$/ Al (NO_3) $_3$/ PVP fibres were observed to be amorphous before heat treatment. The complete decomposition of the bonding polymer, zirconium and aluminium salts at 500°C did not affect the crystal structure of the filaments.

D. Li and co-workers [141] obtained CuO nanostructures prepared by chemical methods. They investigated the influence of synthesis conditions on the morphology of CuO nanostructures. They found that the concentration of the solution, its pH value, the synthesis temperature and the presence of crystals significantly affect the morphology obtained, as well as the adhesion to the substrate. In the absence of crystals and for low solution concentrations, spherical assemblies of CuO slides are obtained. On the other hand, the synthesis of solutions with higher concentrations allows the manufacture of nanostructured films on the substrate, whose morphology and adhesion to the substrate depending on the pH value and the synthesis temperature.

Xiaonong Cheng et al. [143] studied the modifying effects on the chemical reduction synthesis of nanostructured copper. With the pure nanostructured phase of different particle sizes and medium-size distributions, it can be conveniently synthesized starting from copper sulphate using SDBS, SDS, PEG or their mixture as a modifier and ascorbic acid as a reductant. The coordinating interactions between the modifiers and the resulting nanostructure are asserted by FTIR analyzes. The stabilizing capacity of PEG on nanostructured Cu is first increased and decreased with an increasing relative mass of PEGs. The synergistic effects of mixed SDBS or SDS and PEG modifiers on nanostructured Cu stabilization are different from those of an SDBS, SDS or PEG.

G. Xu et al. [144] analyzed the steric effect of PVP and adsorption on ZnO and/ or precursors to obtain a controlled growth in the [0 0 0 1] direction of ZnO nanotubes and nanoparticles at 100°C, and, respectively, 140°C in solvothermal synthesis. Polyvinylpyrrolidone (PVP) has a ring opening reaction to produce PVAB at 120°C and complexation between the groups of asynthesized PVAB carboxylic acid and the Zn(OH) precursor, caused by abnormal growth of ZnO pyramids and the formation of flower-like structures. The results of TEM, SAED, HRTEM, FT-IR, ^{1}H RMN and TGA confirmed the morphology and microstructure of ZnO nanomaterials. The fine ZnO regulation conditions assembled by PVP/ PVAB can lead to distinct structures covering nano and micro dimensions.

Tomasz Tanski et al. [145] obtained thin composite nanofibers with a polyvinylpyrrolidone (PVP) matrix and reinforcement phase in the form of silicon oxide (SiO_2) nanoparticles. The colloidal suspension produced was subjected to a drying process and a calcination process at 550°C, resulting in an amorphous silica nanopowder with an average particle diameter of 20nm. The morphology and structure analysis of the resulting particles, performed based on high-resolution images using electron microscopy and an X-ray diffractometer, showed that the resulting amorphous powder consists of silicon oxide nanoparticles with an average diameter of 23nm. The obtained particle size is particularly beneficial in the use of silicon oxide nanopowder in the biological zone for in vitro contrast imaging of cells. The analysis of the obtained fibre morphology performed based on the image of the surface topography of the fibres obtained using scanning electron microscopy showed a decrease in fibre diameters from 1164 to 358nm due to the presence of silica particles in solution, which can increase the efficiency of filters and sensors with this type of materials. The performed UV-Vis analyzes and the forbidden energy areas of the produced materials specified on these analyzes prove the obtaining of a pure amorphous SiO_2 nanopowder, characterized by a forbidden band of 5.5eV, as well as the obtaining of fibrous PVP. SiO_2 materials are characterized by improved absorption of radiation in the ultraviolet range and at the same time maintaining a good ratio in the radiation range absorbed by the matrix material.

Przemysław D. Gacia et al. [147] performed a low-temperature synthesis of copper oxide (CuO) nanostructures. The researchers demonstrated the low-temperature formation of high-surface CuO nanostructures and studied the effect of temperature on the morphology of the resulting CuO nanostructure. In addition, they investigated the influence of CuO morphology on the specific surface of the different structures obtained. Due to the fine structure and increased availability of surface adsorption sites, the CuO nanostructure with fibrous morphology displayed a large surface area of $179m^2g^{-1}$, a much higher value than CuO nanostructures prepared by other methods. Electrochemical studies have shown that this CuO nanostructure exhibits pseudo-capacitive behaviour with a specific capacity of approx. $28.2Fg^{-1}$ at a scan speed of $5mVs^{-1}$.

A. Lakshmanan and colleagues [152] prepared $Zn/Cu/Al_2O_4$ nanoparticles by the microwave-assisted combustion method to analyze the effect of fuel content on the nonlinear optical and antibacterial activities of these nanoparticles. In SEM images, slight morphological differences in different agglomerated dimensions covered by smaller particles due to fuel selection were observed. Following the analysis of dispersive energy X-ray spectroscopy (EDAX), the content of Zn, Cu, Al and O was found to differ with the fuel/oxidant ratio. Moreover, the atomic ratio decreases significantly with increasing fuel/oxidant ratio.

Hung-Hua Sheu and co-workers [153] studied the effect of the rotational speed of an electromagnetic stirrer on the size of nanoparticles of yttrium-aluminium-garnet (YAG) doped with neodymium (Nd) during co-precipitation. The nanoparticles were synthesized at different rotational speeds of the electromagnetic stirrer with different concentrations of precipitating agent and subjected to a calcination heat treatment at different temperatures. The researchers found that at a rotational speed of 400rpm of the electromagnetic stirrer, small particles of about 300nm can be obtained. The results also indicate that the precursors synthesized at 400rpm can better obtain a pure phase than those prepared at 200 and 300rpm, respectively, subsequently being calcined at temperatures from 800 to 1000°C. Moreover, a laser system made of high-quality Nd:YAG nanopowders can be applied to the manufacture of microelectromechanical devices.

Liu Faxian and co-workers [154] obtained silver nanoparticles by microwave-assisted synthesis and aimed at improving the surfaces intended for their investigation by Raman spectroscopy ("Surface Enhancement Raman Scattering - SERS"). The researchers found that as the reaction time increases, the size of the silver nanoparticles increases. The intensity for surface enhancement by Raman signal scattering (SERS) could be increased by silver nanoparticles. The silver nanoparticles reacted for 15 minutes to the strongest SERS signal. The size and distribution of silver nanoparticles play a very important role in improving the SERS signal. This method can open more efficient and convenient ways to make highly active SERS substrate.

Manabendra Chandra et al. [155] reported the first hyperpolarizability of copper nanoparticles in organic media with and without stabilizer. The 9nm copper nanoparticles were prepared by laser ablation of a copper metal sample, immersed in isopropanol both in the presence and absence of polyvinylpyrrolidone (PVP). They observed that the use of polyvinylpyrrolidone plays a significant role in improving the first hyperpolarizing capacity of noble metal nanoparticles.

Prahlad K. Baruah et al. [156] obtained Cu and Cu_xO nanoparticles synthesized by pulsed laser ablation of a copper target immersed in distilled water. The blue change in the plasmonic peak and the widening of the bandwidth indicate a reduction in the size of the nanoparticles, being confirmed by TEM (Transmission Electron Microscopy) studies. These results were explained using the quantum closure effect, as well as the Mie theory. The structural characteristics of nanoparticles, as revealed by SAED (Electron Diffraction on Selected Area) and Raman studies, suggest that the more oxidized phases of copper nanoparticles are favourably formed with increasing laser ablation and laser energy. Thus, the simultaneous control over the size, the SPR (Surface Plasma Resonance) and the oxidation state of the nanoparticles obtained by varying the duration of laser ablation and laser energy was established.

Songlin Yang and his collaborators [157] deposited YBCO nanoparticles on graphene nanofoils using the MAPLE method (matrix-assisted pulsed laser evaporation). They used a 532nm pulsed Nd:YAG laser to deposit YBCO nanoparticles on graphene nanofoils. The researchers found that by adjusting the irradiation time, they could control the amount of YBCO nanoparticles deposited. The average size of YBCO nanoparticles decreases as time increases. The MAPLE process can maintain the structures and chemical composition of the target materials/molecules without introducing additional chemical reagents.

P.V. Kazakevich et al. [158] synthesized nanoparticles in liquid by laser ablation. They found that the method of laser ablation in a liquid medium is a simple and efficient technique that allows the generation of large amounts of nanoparticles in the form of a suspension in a given liquid. This technique has certain flexibility in controlling the properties of nanoparticles by the appropriate choice of both laser parameters and the nature of the liquid. Laser ablation in a liquid medium is capable of producing nanoparticles without any surfactants or counter-ions, which is indispensable for some applications, for example for medical ones.

Takeshi Tsuji et al. [159] prepared silver nanoparticles by laser ablation in polyvinylpyrrolidone solutions. They performed laser ablation of silver plates in PVP solutions and secondary laser irradiation on the resulting colloids. The results showed that the formation efficiency and stability of the nanoparticles obtained in PVP solutions were improved compared to those obtained in pure water. However, the decrease in size attributed to protection by PVP was smaller through the laser ablation process than through the secondary laser irradiation process. The results of observing the image of the laser ablation process suggested that the increased efficiency of the formation was due to the increase of the efficiency of the secondary ablation process in the PVP solution. The particle size was less affected by PVP in the laser ablation process than in the secondary laser irradiation process because the formation of nanoparticles takes place mainly in the cavitation flask.

ME. Gondal et al. [160] obtained copper oxide nanoparticles produced by the method of pulsed laser ablation and studied the effects of the oxidizing medium on their composition, morphology and optical properties. The authors used liquid pulsed laser ablation (PLAL) with a 532nm wavelength laser with a pulse duration of 5ns to produce the copper oxide nanostructure. The effects of oxidizing media (deionized water and hydrogen peroxide) on the composition, morphology and optical properties of the product was studied. XRD and TEM studies indicate that, in the absence of hydrogen peroxide, the material produced is in two phases (Cu/Cu_2O) with the structure of spherical nanoparticles, while in the presence of hydrogen peroxide in the liquid medium, the produced material revealed two other phases (Cu/CuO) with nanotube-like structure. Optical studies have shown a considerable change in red (3.34-2.5eV) in the band gap energy in the case of liquid hydrogen peroxide in PLAL synthesis compared to that in its absence. Also, the material produced in the presence of hydrogen peroxide in the liquid medium showed a low photoluminescence intensity which indicates a low recombination rate of the electron gaps. The red change of bandwidth energy and the low speed of recombination of electrons make the produced material an ideal photocatalyst for harvesting solar radiation for various applications. The most relevant signals on the FTIR spectrum for samples are the absorption bands in the region between 450 and 700cm^{-1}, these are the characteristic bands of the oxygen bonds with copper. The reported approach on laser ablation for the synthesis of Cu_2O and CuO nanoparticles has the advantage of being a clean method that ensures the control of the obtained particle properties.

Jiaxin Yua et al. [161] studied the control of nanoparticle size by the multi-pulse laser ablation method. The researchers observed that after extending the ablation time from 1h to 16h, although the peak SPR (Surface Plasmon Resonance) is slightly changed to blue, the A450/ASPR ratio is low, which is attributed to an increase in the average nanoparticle size. This result contradicts previous research, in which ablation with a longer time led to the decomposition of manufactured nanoparticles. The authors obtained nanoparticles by single-pulse ablation, with much larger average dimensions (ie >100nm). It was also observed that due to their relatively large size, the manufactured nanoparticles also experienced slow precipitation over several months.

M. Saito et al. [163] fabricated copper nanoparticles by the method of laser ablation in polysiloxane. The researchers used polysiloxane oil to prevent oxidation and aggregation of Cu nanoparticles. The TEM analysis revealed that the Cu particles obtained in the oil have dimensions between 2nm and 20nm. Both particle size and production efficiency have changed, especially depending on the type of oil.

A.A. Menazea [164] used the laser ablation method to synthesize a compound consisting of polyethylene oxide, polyvinylpyrrolidone and copper oxide nanoparticles. FE-SEM scans show a clear change in the morphology of the prepared samples confirming the doping of CuO NPs at the surface. PEO/PVP/CuO prepared NPs were studied by XRD, UV-Vis, PL, SEM and AC conductivity. XRD and SEM confirm the complexation between CuO NPs and the PEO/PVP matrix. The appearance of the characteristic absorption peak at 275nm in the UV-Vis spectrum was attributed to the surface plasmon resonance (SPR) of CuO NPs. The values of the direct and indirect optical band interval show a decrease after the coupling of the PEO/PVP matrix by CuO NPs. PL analysis confirmed that the existence of CuO nanoparticles comprehensively rearranges the delocalized n-electron system of the PEO/PVP mixing matrix. AC (alternating current) conductivity values are increased with increasing laser ablation time.

Zaydoon T. Mohammed Noori et al. [165] fabricated Cu_2O nanoparticles by liquid laser ablation, the phase method (PLALP). The laser ablation method has proven to be one of the most effective physical methods for obtaining copper oxide nanopowders. Using this method, the authors observed that the absorption peak of nano-copper colloids synthesized in the liquid is located at 588nm. The plasmon resonance emission showed the colour green. Both the particle size and their distribution showed particles obtained in different sizes between 100 and 350nm with a bandwidth value of 2.3eV.

Paul N. Barnes and his colleagues [166] obtained YBCO nanoparticles by the pulsed laser deposition (PLD) method. They demonstrated that it is possible to synthesize nanoparticles from YBCO by PLD. The main change was the background pressure of oxygen and the energy of the laser. YBCO nanoparticles are formed only under conditions of high oxygen atmospheric pressure with a low fluidity laser, an assembly that ensures low visible exposure.

Inayah Mumpuni Budiati and collaborators [167] studied the effect of the solvent in the colloidal synthesis of copper nanoparticles by the impulse ablation method. They found that the variation of the distilled water solution, 0.5mM, 5mM and 10mM PVP obtained the most stable colloid at a concentration of 5mM. Based on the results of the UV-Vis test in the spectrum of 292nm - 306nm, the presence of Cu NPs is observed, but it has a different adsorption peak. The results of the XRD analysis show the presence of diffraction peaks, the nanoparticles produced in this study contain CuO compounds.

Rajesh Rawat et al. [169] studied the effect of solvents on the morphology and stability of Cu/CuO nanoparticles synthesized by high-flux laser ablation. They used the 1064nm laser pulsed ablation method and a high laser flux of 40 J/cm^2 (which works for a pulse duration of 8ns). The optical characterization of the sample showed the presence of oxides in all cases. Observing the sample for a longer time, the authors saw the effect of the polarity and dielectric constant of the solvents. The crystallinity of the nanoparticles was confirmed by ^1H RTEM, SAED and XRD analyzes.

The above are probably the most important steps taken by scientists in search of new solutions to old problems: cheap materials, materials with controllable properties, materials with extraordinary properties (mechanical strength, thermal resistance), materials with a very high quality/price ratio. Last but not least - materials that reduce their impact and the industries in which they are applied to the environment.

Conclusions

- efforts to develop nanostructured polymeric materials have attracted a great deal of attention due to the growing importance of these materials in engineering industries such as the aerospace industry, the food industry or biomedical applications;
- recent and extensive reports on the development of preparation methods that can lead to the production of various nanostructured polymeric materials, including micelles, nanoparticles, nanocapsules, nanogels, nanofibers, dendrimers and nanocomposites, have been presented to provide an insight into the complexity of the field and the diversity of approach methods;
- the internal properties of the materials, such as solubility, polymer-load interactions, polymer chain flexibility, surface loading, stereochemistry, surface chemistry, molecular weight and crystallization capacity, etc., must be taken into account when choosing the appropriate preparation method and for proper processing;
- the design of polymer blends is an interesting alternative for obtaining micro and nanostructured surfaces;
- the cost is reasonable and does not contain time-consuming procedures;
- two main aspects must be taken into account when preparing multi-structured mixtures: the interfaces involved and the morphology to be obtained;
- the control of these two aspects still depends on the parameters of the materials involved in the composition of the mixture, the interfacial tension or viscosity ratio and the processing conditions related to the temperature, mixing time or intensity, etc.;
- to date, most studies on polymer blends have been related to the control of physical and chemical properties, their barrier properties or electrical conductivity;
- from the data presented, it appears that by ensuring a rigorous control of polymer nanostructuring and/or adding nanoparticles in polymer matrices, improvements in structural and functional properties can be achieved in a significant number of polymeric systems in response to the continuing requirements of advanced industrial sectors;
- the availability of new nanoparticles with extraordinary properties (ie carbon nanotubes, graphene, but also nanoclay, nanocellulose, metals and ceramics) determines new and interesting possibilities for a continuous expansion of polymer applications and, consequently, for the expansion of the markets of these materials.

2. Objectives

When analyzing the literature, we noticed that complex polymeric nanostructures arouse special interest due to adjustable physico-chemical properties, such as catalytic activity, high sensitivity, electrical and thermal conductivity, scattering properties. Currently, obtaining a nanostructured polymer matrix is a fundamental challenge for the field of polymer materials science and nanotechnology.

Researchers used different methods to obtain nanostructured polymeric materials. The most used methods are gel method, electrospinning method, template synthesis method, phase separation method, self-assembly, *bottom-up* method and *top-down* method, etc.

The main objective of this study is to investigate the possibility of nanostructuring an epoxy system (Epiphen RE 4020/DE 4020) by obtaining, directly in the matrix, complex inorganic oxide structures from metal salts and using 1 methyl-2-pyrrolidinone (NMP) as the solvent.

The achievement of the expected results must be investigated. An analysis of the experimental results regarding the properties of the obtained materials is also necessary as the achievement of the objective may lead to a depreciation of the known properties of epoxy resins. For the study presented in this paper, two objectives were defined:

1. Testing the hypothesis of obtaining nanostructures (complex metal oxides) by possible local chemical reactions carried out in the volume of epoxy resin and the effect of these nanostructures on the mechanical properties of polymeric materials.
2. Formation of YBCO nanostructures in epoxy resin by stimulating the development of local chemical reactions in epoxy resin and the effect of their formation on the mechanical properties of the polymeric materials obtained.

For the first objective, the following partial objectives have been defined:

- establishing the optimal solvation conditions for each type of metal salt;
- establishing the strategy of uniform distribution of the metal salt solution in the epoxy resin;
- determining how to mix epoxy resin mixtures with solutions of metal salts to ensure possible chemical interaction;
- establishing the casting method and the shape of the mould to ensure the necessary specimens required by the characterization of the formed materials;
- formation of control materials;
- formation of epoxy composites modified with NMP solvent;
- formation of epoxy composites modified with inorganic salts;
- analysis of the influence of the applied external magnetic field during the polymerization on the properties of the formed materials;
- analysis of the mechanical properties of the formed materials;
- electrical characterization of the formed materials;
- thermal characterization of the formed materials;
- Raman analysis of materials;
- SEM analysis of materials.

Given that the first objective was investigative, the second objective defines several conclusions related to the achievement of the anterior objective.

- establishing the strategy for solvating inorganic salts in NMP;
- establishing the strategy for stabilizing inorganic salt solutions in NMP;
- establishing mixing strategies between inorganic salt solutions and epoxy resin;
- testing the hypotheses regarding the favouring of the desired chemical reactions for obtaining the complex metal oxide - IR irradiation, blue irradiation, electrolysis in an alternative electric field;
- formation of materials;
- analysis of some mechanical properties of the obtained materials;
- calorimetric analysis of the formed materials;
- Raman analysis of the formed materials;
- SEM analysis of the formed materials.

To validate or invalidate the working hypotheses, an experimental investigation of the formed materials is necessary (as can be seen from the analysis of the partial objectives defined for the two fundamental objectives) and, for this, the following objectives were targeted:

- performing the test pieces necessary to perform all the tests;
- establishing the optimal number of tests for each analyzed property;
- making special moulds (for the study of electrical conductivity and the study of the effect of the presence of the external magnetostatic field on the properties of materials);
- SEM analysis of the materials obtained to identify possible nanostructures formed;
- Raman analysis of materials formed to identify specific chemical bonds for nanostructures (metal oxides);
- calorimetric analysis of the formed materials - with the establishment of the analysis strategy and the thermal fields of interest and, especially, the identification of the substance losses;
- thermomechanical analysis of the formed materials - with the establishment of the analysis strategy and the thermal fields of interest;
- analysis of the electrical conductivity of the materials formed using the method of insulation resistance;
- analysis of mechanical properties - tensile tests - for formed materials;
- interpretation of the results obtained;
- establishing the conclusions and the strategy to be followed for refining the process.

3. Epoxy resin modified with PVP/NMP solution

The first objective of the study was to obtain metal oxide nanostructures directly in the volume of the polymer (epoxy resin) based on the gel method, well known for obtaining nanostructures (either in the version of citrate gels or in the version of oxalic gels). The two methods cited have already been used at CCDCOMT, with promising results. What is significant is that the use of citric acid, respectively oxalic acid, has a double valence: on the one hand, it ensures the formation of gels (from solutions of metal salts) and, on the other hand, it ensures an important discharge of energy at the time of combustion, providing the necessary for the interactions that lead to the formation of complex metal oxides.

Previous studies at CCDCOMT have shown [171] that certain salts can be solubilized in commercial solvents, solutions mixed in RE4020, followed by the removal of the solvent by vaporization and thus the retention of metal ions or dichromate ions in the organic mixture which forms the basis epoxy system.

Also, previous studies developed at CCDCOMT [172], showed that the resins can be modified by using organic solvents: NMP, 1-4 dioxane, N, N dimethylformamide, etc. The cited study also analyzes epoxy mixtures with polysulfone solution in NMP with effects on the properties of materials obtained by mixing an epoxy resin with specified amounts of solutions (polysulfone, NMP).

3.1. Materials

3.1.1. Epoxy resin

The formation of polymeric materials was performed using the EPIPHEN epoxy system composed of RE4020 resin (bisphenol A) and DE4020 hardener (modified aliphatic amine). This epoxy mixture polymerizes at room temperature, has high corrosion resistance, high adhesion to most types of immersed agents for the formation of composites (powders, balls, fibres). Among the properties of this epoxy system are also high mechanical strength, high dimensional stability, dielectric properties.

3.1.2. 1-Methyl-2-pyrrolidinone solvent

1-methyl-2-pyrrolidone (NMP) is a colourless solvent with a boiling point of 202°C and a low viscosity. NMP is known for its low toxicity and solvating power, it is a liquid with a polar nature and has the potential for use in the process of separating polar substances from non-polar substances. It is a useful solvent in most scientific fields, mainly due to its advantages in terms of ambient temperature stability, low volatility, low flammability and industrial use in the field of polymerization, petrochemical processing, surface coating and plastics industry [173], [174].

Uses of NMP include petrochemical processing (acetylene, butadiene, lubricating oil), polymer synthesis (polyethersulfones, polyimides, polyamides), solvent (for resins, paints, adhesives, cleaning agents) and the manufacture of graphene and lithium-ion batteries [181].

3.1.3. Polyvinylpyrrolidone

Polyvinylpyrrolidone (PVP) is a crosslinked homopolymer (formed by polymerizing a single monomer) of pure vinylpyrrolidone [182]. PVP has a high polarity, being a proton acceptor and is amphiphilic [183].

Polyvinylpyrrolidone is soluble in water and other polar solvents, insoluble in esters, ethers, ketones and hydrocarbons. The K values assigned to the different degrees of PVP represent a function of the degree of polymerization, the average molecular weight and the intrinsic viscosity. It has a high degree of compatibility in both film and solution, with natural and synthetic resins, most inorganic salts and many other chemicals [185], [186].

Polyvinylpyrrolidone is a versatile ingredient used in pharmaceutical, cosmetic, industrial production, biomedical applications as a plasma substitute, as binders in pharmaceutical tablets, in hydrogels for wound dressings and disinfectants [187] - [189].

3.2. Materials preparation

In the *first stage* of the research, a study was performed to determine the effect of the presence of solvent and thermoplastic polymer inside the epoxy matrix. Four materials were formed for this study. Cylindrical polypropylene tubes with a diameter of 8mm and a length of 220mm were used as moulds. The reference material was composed of epoxy resin RE4020 and hardener DE4020 with the ratio indicated by the manufacturer, 100:30. The other three materials were formed using the same epoxy system RE4020-DE4020, which was modified by adding different concentrations of polyvinylpyrrolidone powder and 1-methyl-2-pyrrolidinone (NMP) solvent. The concentration of PVP in the NMP solution is the same for all materials (1g/9ml), but at the level of the final material, the epoxy resin is diluted by the presence of 5%, 10% or 15% of the mentioned PVP/NMP solution.

3.3. Epoxy resin modified with PVP/NMP solution

The experimental results obtained in the analysis of materials obtained by modifying the epoxy resin with the PVP/NMP solution was presented. Thus, the reference material (epoxy resin) is denoted M0 and the specimens were formed as described above using the standard mixture recommended by the manufacturer of the epoxy system Epiphen RE4020 - DE4020, ie 100:30 (volumetric parts - in the case of cm^3). For this material, as well as for the modified ones, 15 cylindrical specimens were formed. To obtain the modified materials from the total amount of epoxy resin, the volume of the PVP/NMP solution was reduced (9ml, 18ml and 27ml, respectively), reducing accordingly the volumes of RE4020 (resin) and DE4020 (hardener). PVP/NMP in the resin is 5%), M2 (10%) and M3 (15% PVP/NMP solution in epoxy resin, respectively).

3.3.1. Mechanical properties of PVP/NMP solution modified epoxy resin

Figure 1 shows the results for five specimens of each material. The observed behaviour of the materials is one of brittle fracture for M0 and M1 (although it can be easily seen that the slopes are different). Ductile rupture for the M2 material was observed and bottlenecks in the engagement area and fracture of the specimens at the neck, i.e. a behaviour similar to thermoplastic polymers. For the M3 material (very soft) very long elongations of the specimens were observed.

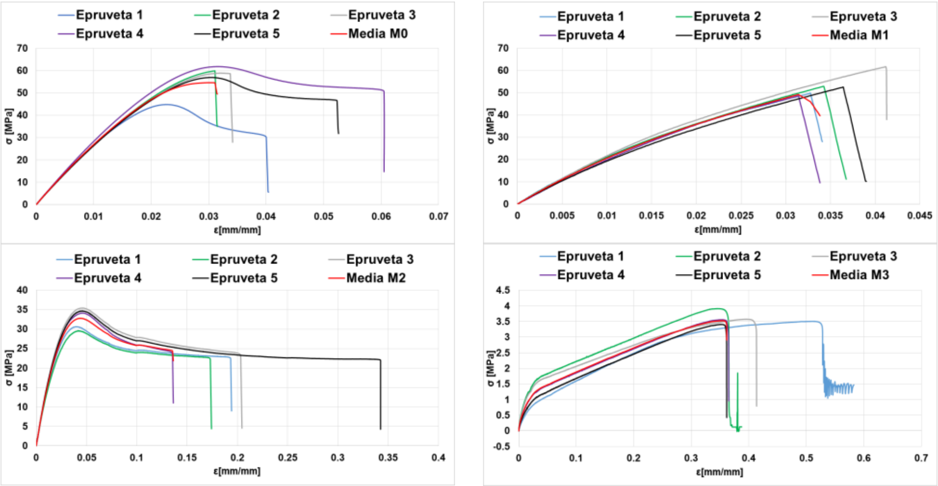

Figure 1. The σ/ε curves for the four analyzed materials

Conclusions

- the modification of the epoxy resin with the PVP / NMP solution (in three different concentrations) significantly modifies the mechanical behaviour of the materials;

3.3.2. Thermal analysis of PVP/NMP solution modified epoxy resin.

Figure 5 shows the segments of interest of the thermal tests performed on the materials obtained by modifying the epoxy resin with PVP/NMP solution - these are the heating segments and the cooling segments, not showing the initial cooling to -60°C or the steps in which the value of the sample temperature does not change.

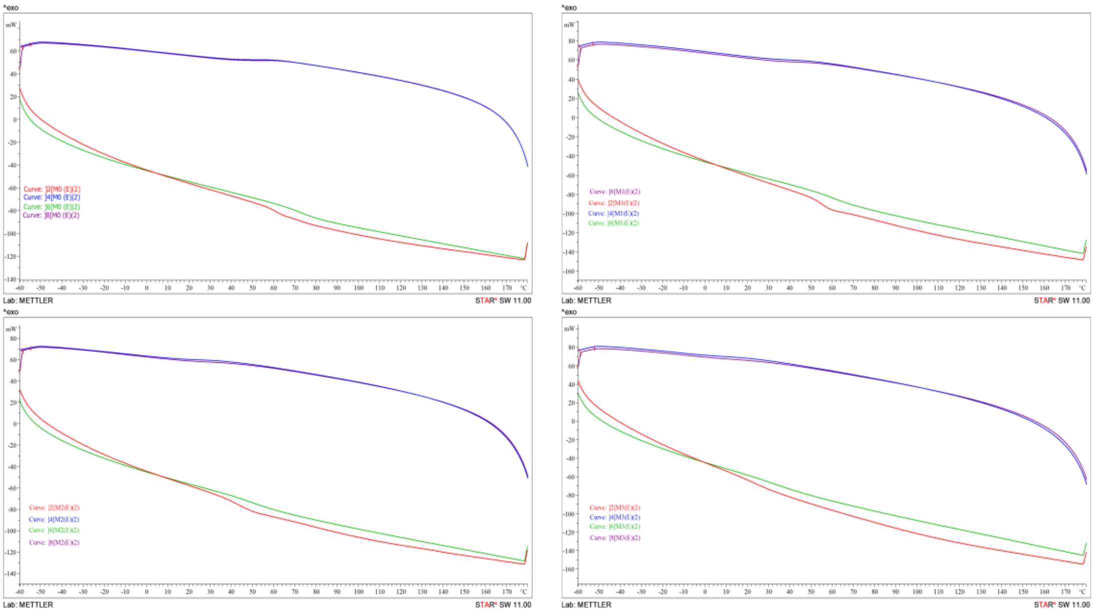

Figure 5. The steps of interest of thermal analysis for M0-M3 materials

Figure 8 shows the temperature variation curves of the specific heat for the analyzed materials. In each case, a slight increase in the values determined on the second cooling (even in the case of unmodified epoxy resin M0) can be observed in the case of low-temperature values and a decrease in the case of high-temperature values. It is also observed that as the share of PVP/NMP solution in the epoxy matrix increases, this transition shifts to the left.

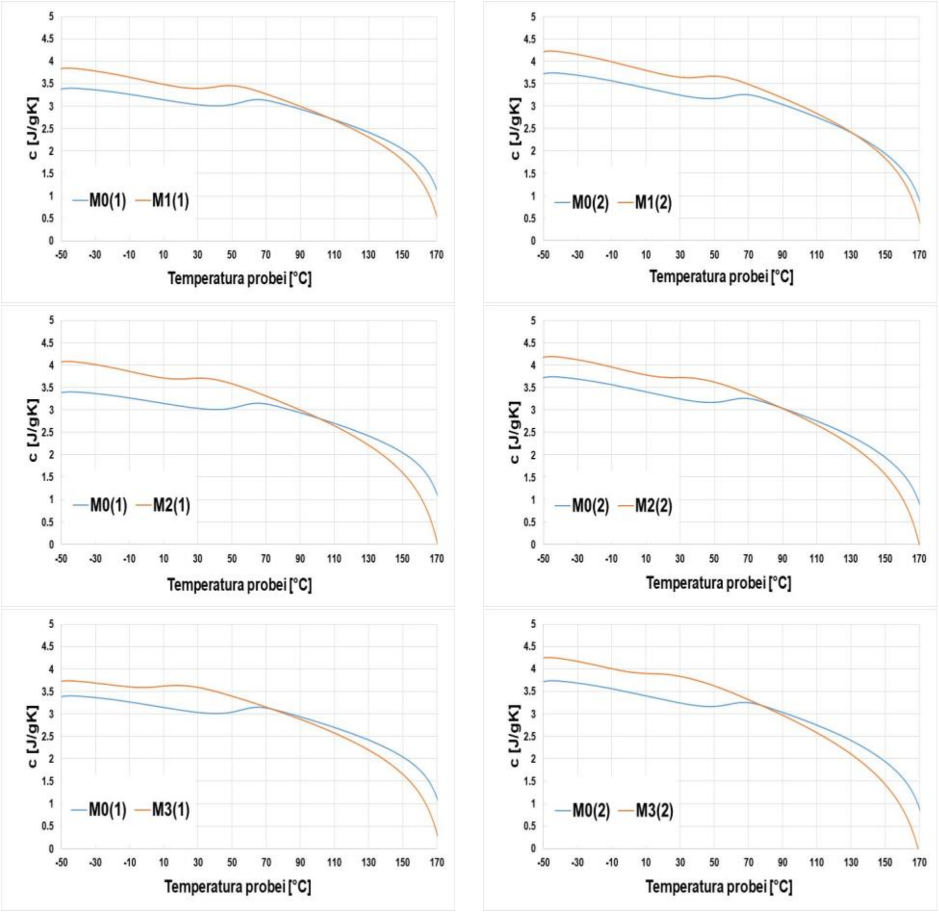

Figure 8. The variation curves of specific heat vs. temperature

Conclusions

- the presence of the PVP/NMP solution in the epoxy matrix causes a shift to low-temperature values of the glass transition temperature value;
- the substance losses found during the test are higher during the first cycle, in the second cycle they are halved;
- Substance losses may be associated with organic agents used as modifying agents (PVP and NMP) although it may be found that epoxy resin has mass losses in the second test cycle, also;

3.3.3. Thermomechanical analysis of PVP/NMP solution modified epoxy resin

In the representations below, all curves start from 0 (zero) because, to ensure the average of the three determinations, the recalibration variant was preferred (in order to avoid the mediation of some curves that do not have the same origin). The material M1 has a value of the coefficient of linear expansion lower than the value of the same parameter determined for the epoxy resin - M0.

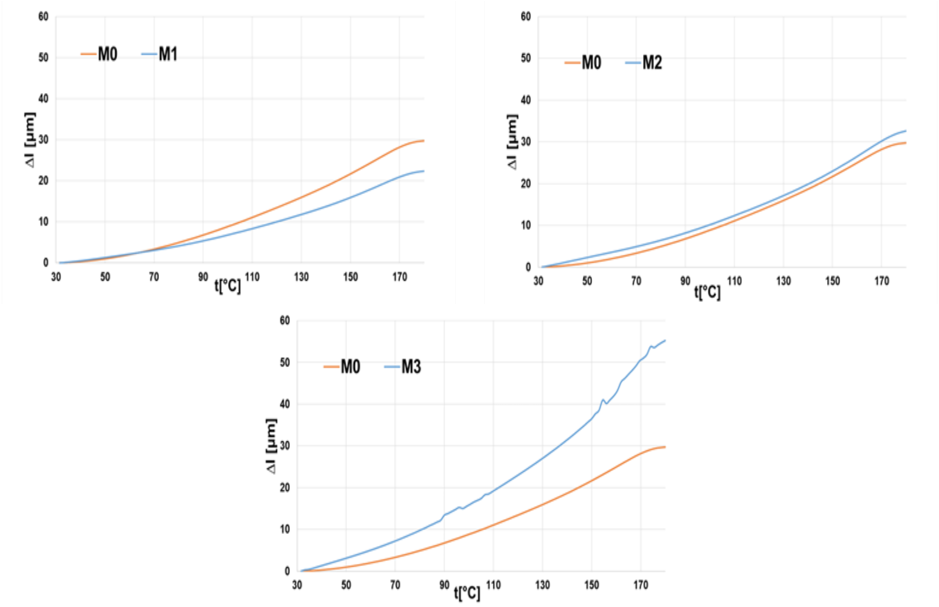

Figure 9. Increasing of the material thickness depending on the temperature value

Conclusions

- M1 material appears to be more stable than the reference material (unmodified epoxy resin);
- the M2 material has a behaviour similar to that of the reference material (curve profile) and even the values of the linear expansion coefficient are close;
- the M3 material is very soft and proves to be relatively unstable.

3.3.5. Raman spectrophotometry for PVP/NMP solution modified epoxy resin

Figure 13 shows the Raman spectra of the modified epoxy resin with different concentrations of PVP/NMP.

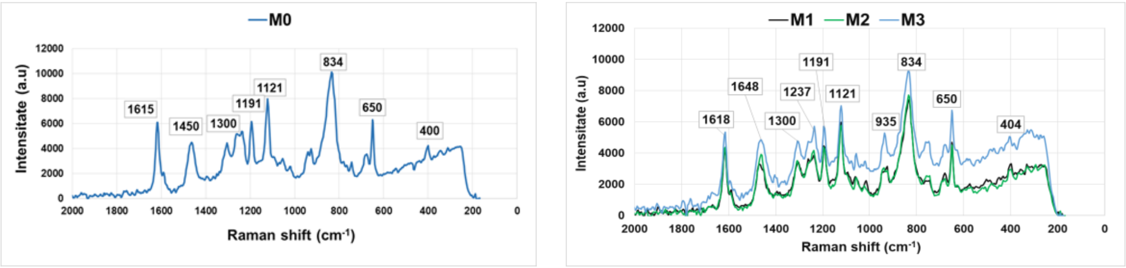

Figure 13. Raman spectra of modified materials (compared to M0)

Conclusions

- no significant changes in the Raman spectrum profile of the epoxy resin are observed (mainly due to the low concentration of the modifying agent, PVP/NMP solution).

4. Epoxy resin modified with inorganic agents solvated in PVP/NMP

The material known as YBCO is a ceramic material (complex oxide) that has electrical superconductivity at relatively high temperatures. However, the choice of this material was determined by the fact that we know it can be formed. Based on the model of this material - $YBa_2Cu_3O_x$ - by analogy, we also tested the obtaining of a $Zr_xBa_yAg_zO_t$ compound. For this, and based on the results obtained at CCDCOMT, we established a strategy based on the use of metal chlorides and a strategy based on the use of metal nitrates. Unlike the study [178], this time, the solvent was to remain in the polymer after its polymerization, the effects of its presence in the study being known [179]. In the following, materials modified with inorganic agents that could lead to YBCO are marked with B while the others are noted with A.

4.1. Materials

The inorganic salts used for the study were purchased from Sigma-Aldrich, as well as the solvent and polyvinylpyrrolidone with the support of *Project 12 P01 024 21 (C11) / 31.08.2012 (SMIS code 50414)*. The epoxy resin used is the one on which most studies were performed at CCDCOMT - Epiphen RE4020 - DE4020 system (*Resoltech SAS*). Solubility tests, performed before starting the formation of materials, showed that nitrates are more soluble than chlorides of the same metals in NMP so the decision was to use nitrates to form modified materials with inorganic and organic agents.

4.1.1. Copper nitrate

Copper nitrate is also found under the name of copper nitrate or copper nitrate. This is a blue inorganic salt, the chemical formula being $Cu(NO_3)_2$. It is obtained by decomposing copper minerals. Copper nitrate comes in four forms: anhydrous, nonhydrate, trihydrate and hexahydrate.

4.1.2. Yttrium nitrate

Yttrium nitrate is an inorganic compound in the form of crystal or powder. Yttrium nitrate dissolves rapidly in most solvents. This compound is used as a laboratory reagent, but also for obtaining electrical components or superconducting materials, being compatible with most nitrates and having a lower pH (acid).

4.1.3. Barium nitrate

Barium nitrate ($Ba (NO_3)_2$) is a colourless crystalline powder. This substance can be used to produce other barium compounds (barium chloride, $BaCl_2$, and barium hydroxide, $Ba(OH)_2$), but also for the production of fireworks, manufacturing of high-quality glass products with a coefficient of linear thermal expansion small, production of bullets, pH regulators, manufacture of chemicals, minerals and water treatment products.

4.1.4. Zirconium oxynitrate

Zirconium oxynitrate is a white substance that is used to prepare mixed oxide catalyst supports of CeO_2-ZrO_2 used for the manufacture of batteries. Its chemical formula is $ZrO(NO_3)_2$. It can be used as a zirconium precursor in the preparation of ferroelectric thin films, nanocrystalline wax/zirconia doped with silicon and alumina ($Ce_{0.5}Zr_{0.5}O_2$).

4.1.5. Silver nitrate

Silver nitrate is an inorganic chemical with the chemical formula $AgNO_3$. Silver nitrate is a colourless or white crystalline solid that turns black if exposed to light or organic materials. It is often used as a precursor to other silver-containing compounds. Silver nitrate is a caustic chemical compound, it is used as an antiseptic, as a cauterizing agent or in the industrial preparation of other silver salts, and as a reagent in analytical chemistry.

4.2. Forming of materials

The design of the research continued in several directions: first of all, establishing the number of specimens required for the tests. The analysis of the results obtained in the first stage confirmed that the use of cylindrical moulds is convenient and cheap provided - already mentioned in the previous chapter - that each specimen is a different material (due to varying formation conditions which is understood as changes in viscosity of the prepolymer mixture). Another issue related to the design of the research was related to the optimal strategy for making mixtures between the epoxy resin and metal salt solutions.

In this regard, two strategies have been established - in the first of them equal volumes of the three salt solutions that could lead to YBCO (B) or ZBAO (A) - where the acronym ZBAO is constructed like YBCO without existing in the literature but which can provide a better picture of the steps taken - they are mixed for 24 hours after which the mixture is mixed with epoxy resin for another 24 hours. After adding the required amount of hardener, followed by a 15-minute mixing, the mixture was poured into moulds. In Table 6 the materials obtained in this way are denoted B(g)Y or A(g)Y, where Y can take the values 3, 6 or 9 and g means global mixture. The second strategy was to mix the necessary volumes of solutions of metal salts in equal parts of resin. The amount of resin required to obtain the projected number of specimens was divided into three equal volumes. The solution and resin mixtures were mixed for 24 hours after which the partial mixtures were mixed for another 24 hours. Thus, finally, after 24 hours for each of the two strategies, the necessary quantities of mixtures containing the same components in the same concentrations were obtained. The materials obtained in this strategy will be marked below with B(s) and A(s) respectively.

Table 1 did not mention materials B(x)9 and A(x)9. They were formed, removed from the moulds and heat-treated but, inexplicably, disappeared from the laboratory before they could be characterized. Their loss is not very important because we already know that, mechanically speaking, their properties are very weak. Each of the formed materials has a correspondent in the materials formed in the previous step A(x)3 and B(x)3 correspond to M1, A(x)6 and B(x)6 correspond to M2 and finally, A(x)9 and B(x)9 would correspond to M3.

Also in the formation of these materials, an attempt was made to obtain specimens that would allow the easier determination of the electrical conductivity of the formed materials. In this sense, moulds were built in which metal pins were placed. After polymerization, these pins remain in specimens ensuring perfect contact with the obtained material.

Table 1 Materials used for the formation of polymeric nanostructures

Sample code	Resin RE4020 [ml]	Hardener DE4020 [ml]	Cu (NO_3)$_2$ +PVP/NMP [ml]	Y(NO_3)$_3$ +PVP/NMP [ml]	Ag(NO_3) +PVP/NMP [ml]	N_2O_7Zr +PVP/NMP [ml]	Ba(NO_3)$_2$ +PVP/NMP [ml]
B(x)3	131,53	39,47	3	3	-	-	3
B(x)6	121,5	40,5	6	6	-	-	6
A(x)3	131,53	39,47			3	3	3
A(x)6	121,5	40,5			6	6	6
M0	135	45	-	-	-	-	-

Also, based on the hypothesis that the presence of a magnetic field could influence the final properties of the materials, a technique was designed to apply a magnetostatic field during the polymerization of the material in the mould. Thus, the first attempt was to close the two ends of the mould with plugs made of magnets (pellet magnets with a diameter of 8 mm or 9 mm). They can be grouped to obtain plugs with the desired height, given that the thickness of each of them is 1 mm. The approach seemed promising, but efforts to control the introduction of plugs have shown that it is almost impossible to maintain the geometry of the plug when closing the mould. That is why this method was replaced by the application of annular magnets on the outside of the moulds - figure 14 (right). From the performed analyzes, we were not able to identify any effect of the presence of the magnetic field.

Figure 14. Test tube with pins (for determining electrical resistance) and moulds with annular magnets

However, the experiments allowed us to find the optimal way to close the moulds - plugs made of metal discs sealed with wax.

Conclusions

- moulds were designed and made to obtain samples to facilitate the determination of electrical resistance of materials (failure);
- moulds were designed and made to allow the application of a magnetostatic field during the natural polymerization of the samples (success) which did not lead to the identification of any effect;
- the optimal method of closing the cylindrical moulds was identified, a method that was also used in the continuation of the study.

4.3. Epoxy resin modified with inorganic and organic agents

Eight materials were formed - using the two proposed strategies (and mentioned above). On the one hand, the *overall strategy (g)* involves mixing individual salt solutions before the mixture is mixed with the resin. On the other hand, the *separate strategy (s)* involves mixing each solution with one-third of the required amount of resin followed by mixing the obtained mixtures.

4.3.1. Mechanical properties of epoxy resin modified with solutions of inorganic agents in PVP/NMP

Figure 17 shows the comparative analysis of the behaviour of the modified material with inorganic agents. Given that there is this major difference between the behaviour of materials modified with inorganic agents, given that the concentration of PVP/NMP is the same as in the case of materials modified with this solution, a first conclusion is that the presence of inorganic agents leads to a dramatic reduction in the mechanical properties of the materials thus formed.

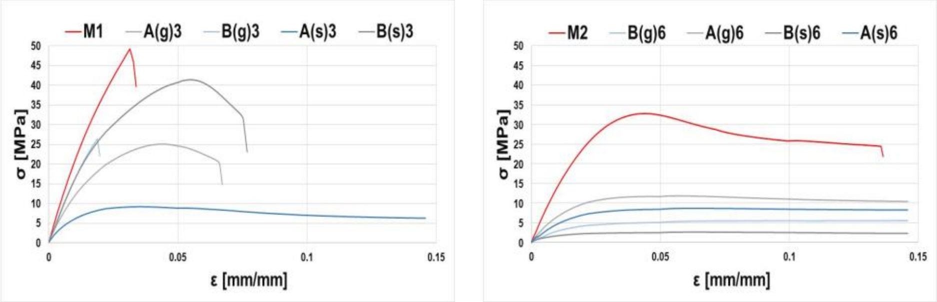

Figure 17. Comparative analysis of the behaviour for modified materials with inorganic agents

Conclusions

- materials modified with 10% solution of inorganic salts in PVP/NMP behave differently in the sense that, for the material modified with silver, zirconium and barium nitrates the separate strategy led to a material with a modulus of elasticity while, for materials modified with yttrium, barium and copper nitrates, the overall strategy led to a material with a higher modulus of elasticity value;

4.3.2. Calorimetric analysis of epoxy resin modified with solutions of inorganic agents in PVP/NMP

As in the case of the materials presented in the previous chapter, the calorimetric analysis aims at determining the specific heat of the formed materials and determining the value of the glass transition temperature. The tests, performed on three samples of each material, followed the same pattern of analysis as those presented in the previous chapter.

The analysis of the data presented in Figures 25 and 26 also reveals that the analogous samples have different behaviour especially in the area of low-temperature values. It is again interesting that during the first test cycle (the value of specific heat determined on the first cooling segment) the analogous materials behave similarly (in all situations) while for the values determined on the second cooling of the materials the behaviour of the analogues is more dispersed. Although there is one exception, materials B(s)3, B(g)3 in which the dispersion is higher in the case of determinations on first cooling.

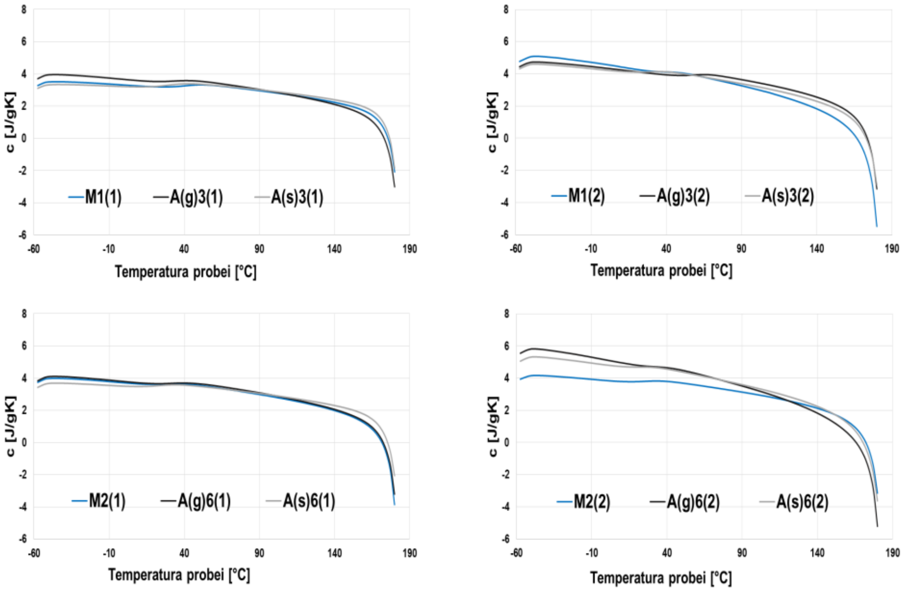

Figure 25. Specific heat as a function of temperature – type- A materials

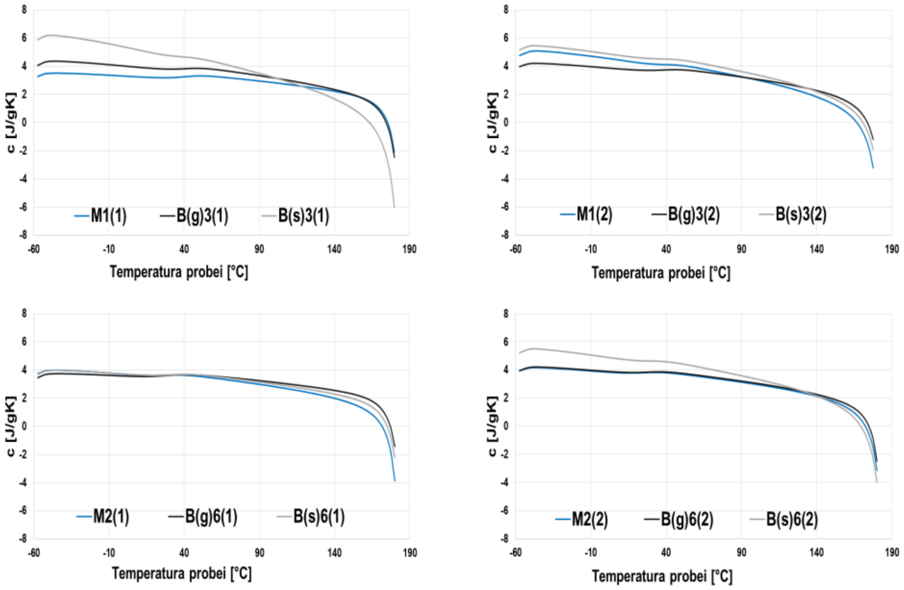

Figure 26. Specific heat as a function of temperature – Type- B materials

Conclusions

- calorimetric analysis of materials modified with solutions of inorganic agents in PVP/NMP indicates slight increases in the specific heat values in relation to the values of the same parameter recorded for the reference materials (epoxy resin modified with PVP/NMP solution);
- for all materials modified with 5% (in epoxy resin) solution of inorganic agents in PVP/NMP the mass losses recorded during the tests were higher than the mass losses of the reference material (epoxy resin modified with 5% solution PVP/NMP);
- for all materials modified with 10% (in epoxy resin) solution of inorganic agents in PVP/NMP the mass losses recorded during the tests were lower than the mass losses of the reference material (epoxy resin modified with 10% solution PVP/NMP);

4.3.3. Thermomechanical analysis of epoxy resin modified with solutions of inorganic agents in PVP/NMP

As in the case of the reference materials, three specimens of each material analyzed were thermomechanically analyzed to determine the coefficient of linear thermal expansion. The results presented below are average values of the results obtained for the three specimens from each material. Each specimen had a thickness between 1.5mm and 2mm. For each test, the determination was scaled so that the software application records the value of the thickness increase and not the thickness (thus it is possible to achieve average curves).

The analysis of the data presented in Figure 29 leads to the conclusion that, regardless of the material formation strategy, materials modified with inorganic agents have diminished dimensional stability compared to modified counterparts with PVP/NMP solution. The only exception is material A(g)6 which has practically the same temperature-dependent expansion curve.

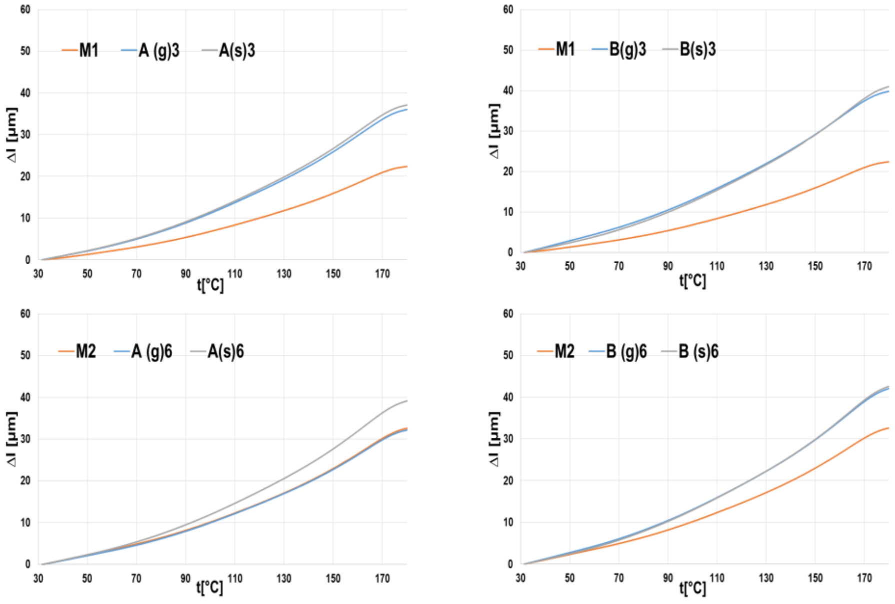

Figure 29. Variation curves of the absolute expansion of the analyzed materials

Conclusions

- the materials modified with solutions of organic agents in PVP/NMP have slightly higher values of the linear thermal expansion coefficient (over the thermal analysis intervals) than their counterparts obtained by modifying the epoxy resin with PVP/NMP solution;
- on the thermal analysis range corresponding to the high values, all materials modified with solutions of inorganic agents in PVP/NMP have values of the coefficient of linear expansion slightly lower than the value of the coefficient of linear thermal expansion of the epoxy resin;
- certainly, the study presented at the end of the previous subchapter could also provide relevant information on the dimensional stability of modified materials;

4.3.4. Raman spectrophotometry of epoxy resin modified with solutions of inorganic agents in PVP/NMP

In the hope of obtaining visible results, Raman spectrophotometry tests of the materials used in the formation of epoxy resins modified with solutions of organic agents in PVP/NMP were also performed. Certainly, even in the case of the existence of signals from C - M or N - M (M metal) bonds, the possibility of visualizing them would be minimal given the low concentration of inorganic agents in the formed materials.

In the following (figure 32), the Raman spectra of the materials analyzed in this chapter are presented. Obviously, the spectra do not contain information on the presence of inorganic agents in the modified epoxy matrix with PVP/NMP solution. Even if there were any trace of the compounds, it would not have been high enough to be observed between the signals of the matrix and the PVP/NMP solution (presented in the third chapter). It is observed that the eight formed materials have common peaks (404, 650, 834, 935, 1194, 1618 cm^{-1}) with the reference materials (M1 and M2, respectively). According to studies by Wang et al. [201], the region between 1200-1400 cm^{-1} corresponds to the presence of azo compounds. Izquierdo and co-workers [202] state that the wavenumber 656 cm^{-1} represents the symmetrical stretching vibrations of the BaO group. In all high spectra, there is a peak of 650 cm^{-1} that can be attributed to these vibrations.

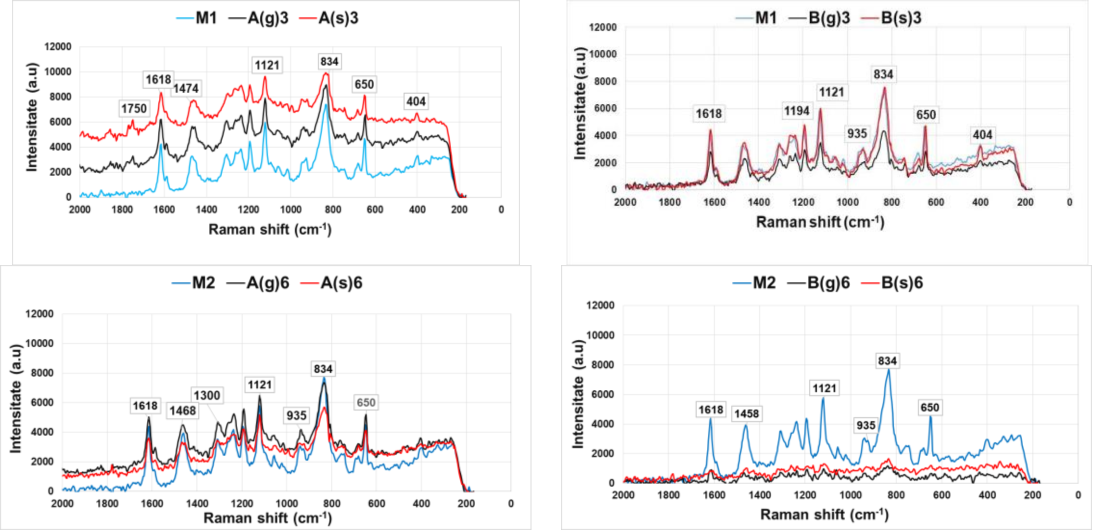

Figure 32. The Raman spectra of materials modified with solutions of inorganic agents

Conclusions

- Raman analysis highlights the reduction of the epoxy resin signal with the increase of PVP/NMP concentration in the matrix;
- due to the low concentration of inorganic agents, not even their presence in the matrix can be highlighted.

4.3.5. SEM analysis of epoxy resin modified with inorganic agent solutions in PVP/NMP

An SEM analysis of the materials formed with the highest concentration of inorganic agents was performed. This analysis aimed to investigate the formation of nanostructures in the polymer matrix and, therefore, was performed only on materials with high concentrations of inorganic agents (higher concentration leads to an increase in the probability of chemical interaction and therefore the possible formation of nanostructures).

In search of possible nanoaggregates, for each of the two materials, two areas were investigated, the SEM images of which are shown in Figures 34 and 35, for material A(g)6 and in Figures 36 and 37, for material B(g)6.

Both in the images in Figure 35 and the following, areas are observed where the density of metals is higher (lighter dots). Their presence is much more important in the case of material B(g)6 but, at this moment, it is only proof that in the epoxy matrix there are agglomerations with nanometric dimensions, but without being able to establish their nature.

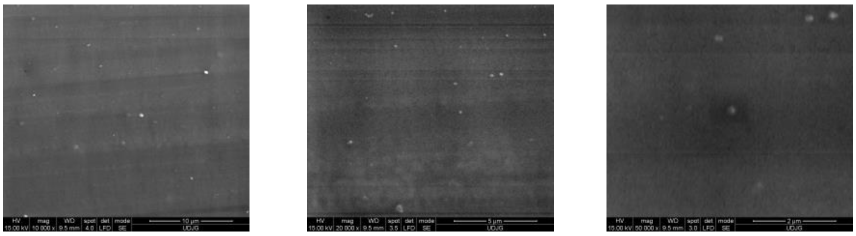

Figure 34. SEM images of the first investigated area of A(g)6 material

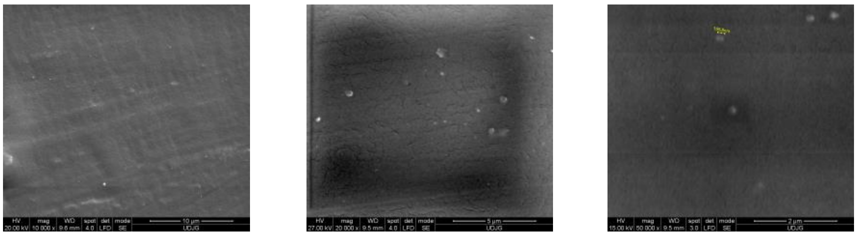

Figure 35. SEM images of A(g)6 material (second investigation area)

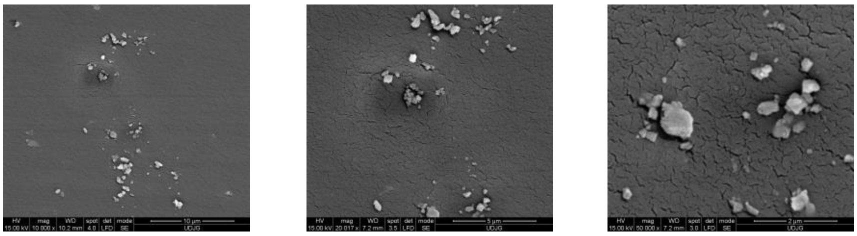

Figure 36. SEM images of B(g)6 material (first investigation area)

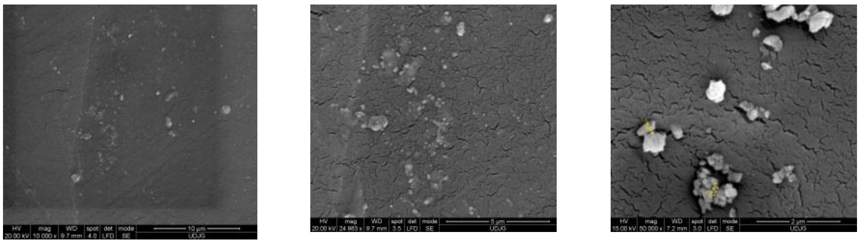

Figure 37. SEM images of B(g)6 material (second investigation area)

For both A(g)6 and B(g)6, measurements of the largest size of some aggregates were made on the last images. Thus, in the case of material A(g)6 the maximum size of 165.8nm of an aggregate were measured, while for material B(g)6 the dimensions of 198.2nm and 203.6nm were measured, respectively. Analyzing these images it is possible to identify a cause of how the fracture of each sample occurred (to obtain the analyzed fragments). In the case of A(g)6, fracturing probably occurred due to differences in the density of the material (at its boundary). In the case of material B(g)6, the presence of a significant number of nanodimensional aggregates was a source of defects in the polymer network with consequences for its mechanical strength.

At this point, it cannot be stated that the intended nanostructures were obtained in the polymer matrix - as they were presented in the first paragraph of this chapter. There are some aggregates with nanometric dimensions - in the case of A(g)6 they have an almost spherical shape and are quite rare and in the case of B(g)6 they are larger and are made up of crystalline-looking groups (edges and flat faces) but this does not mean that intentionally mixed oxides have been obtained. It is possible that some of these aggregates are made by recrystallizing inorganic agents - most likely barium nitrate which was the most soluble gel. To the detriment of this hypothesis, there is the argument related to the different aspect of the agglomerations in the two analyzed materials.

4.3.6. EDX analysis of epoxy resin modified with solutions of inorganic agents in PVP/NMP

As it is very well known, the electron microscope also allows the elementary analysis of the investigated materials - both on certain surfaces and at certain points. The following is largely a search for the nanostructures mentioned above.

4.3.6.1. EDX analysis of A(g)6 material

Figure 38 shows the distribution maps of the elements in a fracture area of material A(g)6. The analysis aimed to identify oxygen, nitrogen, silver, zirconium and barium. The figure below contains information on the distribution of these elements and, as can be seen, carbon was excluded from this analysis. To perform the analysis, the acceleration voltage was 27keV. The investigated area is not related to the area presented in the SEM analysis. For this investigation, the magnification is 10000x.

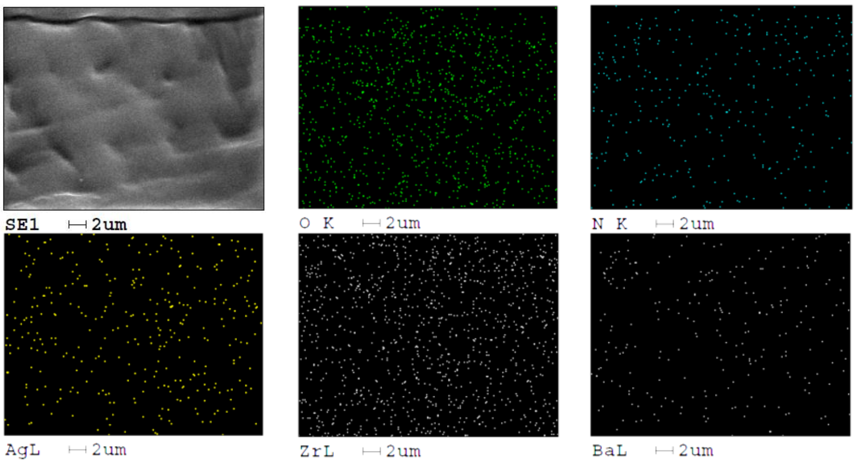

Figure 38. Distribution of elements. Material A(g)6 (10000x)

4.3.6.2. EDX analysis of B(g)6 material

In the analysis of this material, three different magnifications were used in an attempt to identify the possible formation of YBCO nanostructures. Figure 46 shows the map of the distribution of the elements (excluding carbon) for a 10000x magnification. In this case, the analysis is aimed at identifying oxygen, nitrogen, yttrium, copper and barium.

Figure 46 shows the quasi-uniform distribution of the three metals in the polymer matrix.

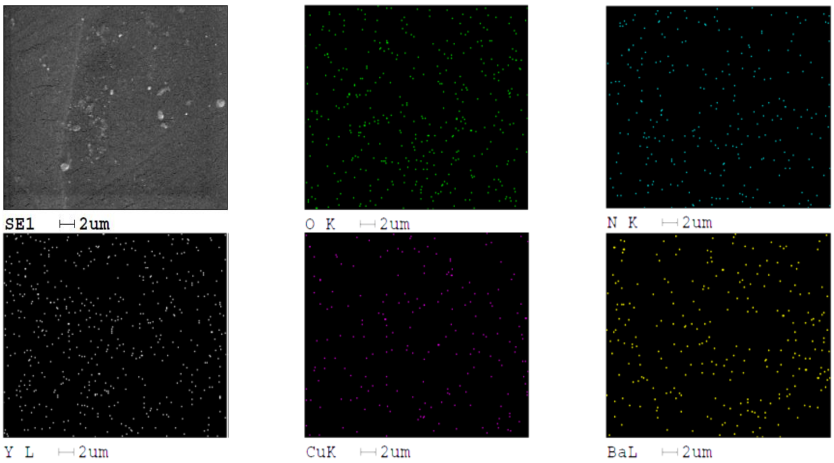

Figure 46. Distribution of elements. Material B (g) 6 (10000x)

Starting from this area, punctual elementary investigations were carried out, which will be presented in the following. Another formatting will be used to limit the space given to images.

Figure 49 showed only once the image of the analysis target but showed the quantitative results for two analyzes - one that includes carbon (and is in the upper right) and one that does not include carbon (lower right). This is only valid for the first point of analysis because for the following analyzes (performed in six other points) the data were presented differently, allowing more efficient use of space.

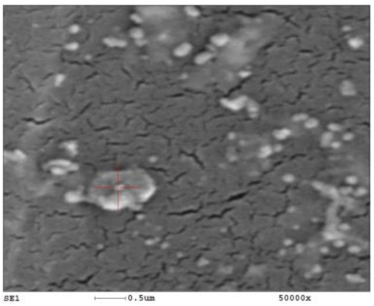

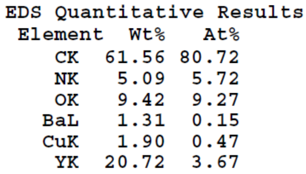

EDS Quantitative Results

Element	Wt%	At%
CK	61.56	80.72
NK	5.09	5.72
OK	9.42	9.27
BaL	1.31	0.15
CuK	1.90	0.47
YK	20.72	3.67

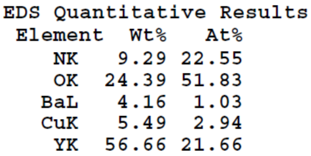

EDS Quantitative Results

Element	Wt%	At%
NK	9.29	22.55
OK	24.39	51.83
BaL	4.16	1.03
CuK	5.49	2.94
YK	56.66	21.66

Figure 49. Punctual elementary analysis - point 1. Material B(g)6 (50000x)

From the experience of colleagues who have presented such analyzes, it is known that, when printed, the images of the distribution maps of the elements do not have a quality that allows viewing (even if in the original file - .pdf - they provide sufficient quality). Under these conditions, each image cropped from the portable file has been slightly processed (in terms of brightness and contrast) to ensure the quality of data visibility - the coloured dots distributed.

Conclusions

- materials modified with silver, zirconium and barium salts do not show - in SEM and EDX analyzes agglomerations of nanometric dimensions except for a few points where only the presence of silver is identified;
- materials to which yttrium, barium and copper salts (nitrates) have been added have agglomerations with dimensions of ordinal nanometers and, in six out of seven points analyzed, all three species of metal atoms are found;

5. Epoxy resin with chemically obtained nanostructures

The study was designed only on the use of yttrium, barium and copper nitrates solvated in the same PVP/NMP solution. This time the goal of obtaining materials with a behaviour similar to epoxy resin or reference materials was less pursued and the emphasis was on the formation of agglomerations of metal atoms. In this sense, the solubilization of metal nitrates was followed by the total solvation of barium nitrate.

5.1. Forming of materials

Three ways of stimulating possible chemical reactions have been proposed. A simple strategy that strictly involves the continuous mixing of the mixture of solutions with the resin, on a magnetic stirrer (300rot/min) at a temperature value of 70°C following that the mixture is maintained in these standard conditions of 24, 48, 72, 96 and, respectively 120 hours before adding the hardener and pouring into moulds. The letter T (thermal) is used to designate these materials and 1 - 24h, 2 - 48h, 3 - 72h, 4 - 96h and, finally, 5 - 120h are used to identify the duration of the preparation. For all materials in this study N (nanostructures) is used so that materials formed in this way will be presented as NT1, NT2, NT3, NT4 and NT5.

A second strategy that, in addition to the conditions from the previous strategy (T) involves exposing the mixture of the solution of inorganic agents with the resin to an electromagnetic exposure at two wavelengths - the strategy is denoted F (photo), and the materials will be noted NF. One of the wavelengths is in the IR range (produces heating), the other is in the visible range (green-blue) and could produce copper nitrate excitation.

The third strategy involves exposing the mixture of the solution of metal nitrates and epoxy resin to the action of a sinusoidal electric field applied for 30 minutes every 24 hours. The strategy is applied under the conditions of strategy T (to which is added the action of the electric field) and the formed materials are denoted NE (electric).

5.1.1. Forming of NT materials

The whole process used to make the test pieces of NT materials is presented in figure 52.

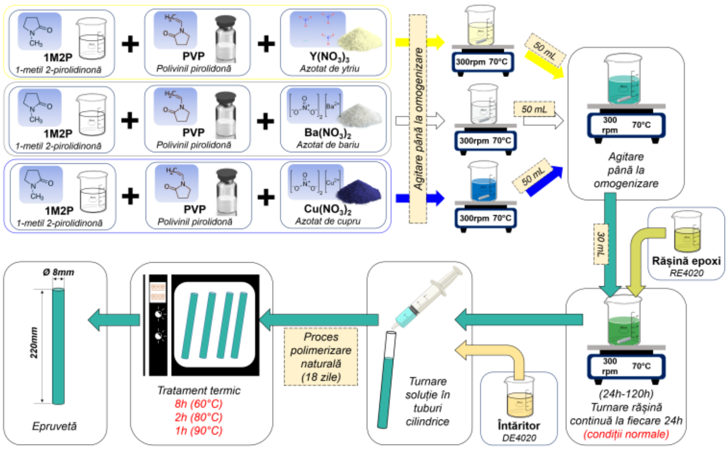

Figure 52. The process of forming NT materials

5.1.2. Forming of NF materials

In the second strategy, the same steps were taken, with the same amounts of compounds. The difference lies in the exposure of the mixture between the mixture of metal salt solutions in PVP/NMP to electromagnetic radiation in the IR range and visible (green-blue). The complete process for forming NF material specimens is shown in Figure 54.

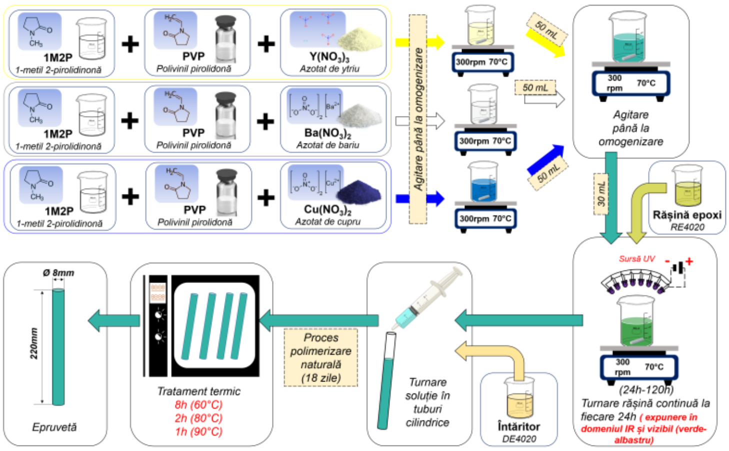

Figure 54. The process of forming NF materials

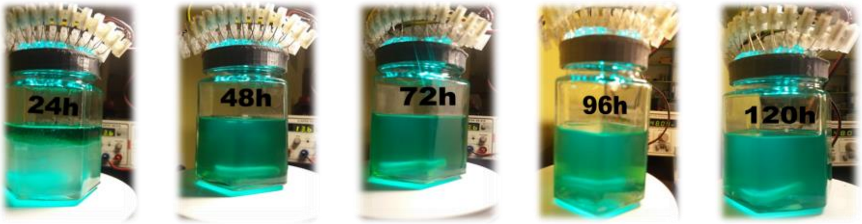

Figure 55. The appearance of the pre-polymeric mixture (NF) before the addition of the hardener

5.1.3. Forming of NE materials

The third strategy follows the steps, the amounts of compounds and the time intervals for placing the mixtures in the moulds, as in the first two methods. Here, the difference is the applying of an alternating sinusoidal electric field (frequency 30kHz, voltage: V_{pp} = 40V) every 24 hours, for 30 minutes, for each mixture. Figure 57 also shows the copper electrodes used for this purpose.

Figure 56 shows the entire process of obtaining specimens of NE type materials.

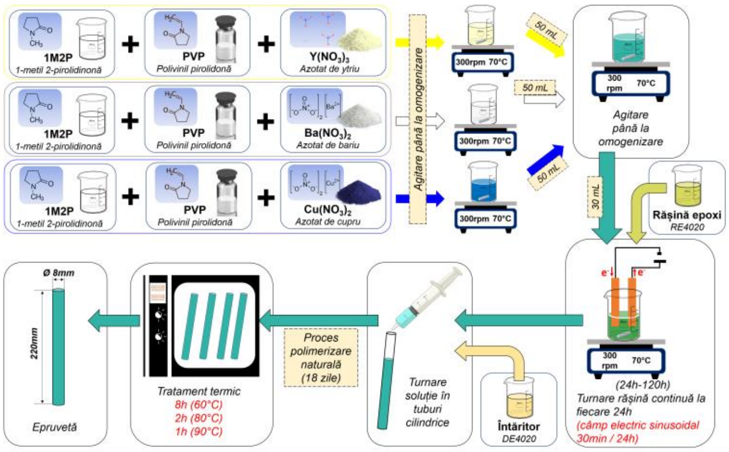

Figure 56. The process of forming NE materials

Figure 57. The appearance of the pre-polymeric mixture (NE) before the addition of the hardener

5.2. Analysis of mechanical properties of N materials

This is why the properties analysis of the materials formed in this study will be done by reference to the properties of the M3 material. The materials are now formed to test the hypothesis of favouring or stimulating any chemical reactions leading to the formation of YBCO-type nanometer-size agglomerations. To increase the concentrations of nitrates and to stabilize their solutions in PVP/NMP this compromise (of increasing the concentration of PVP/NMP) in the epoxy matrix was made but this does not mean that the materials were not analyzed.

5.2.1. NT materials

Figure 58 shows the stress-strain curves for NT materials. Most tests have a wavy tail that proves the previous statement. Analysis of the data in Figure 58 confirms the assumption that N-type materials (in this case NT) have a lower mechanical response than the reference material - M3. The only exception to small deformations is the response of the NT1 material. The NT3 and NT4 responses are similar, with a slight superiority in the case of NT4. NT5 has a superior response even to NT2 but, like this one, it seems to leave the elasticity zone at the same deformation as M3 and NT1.

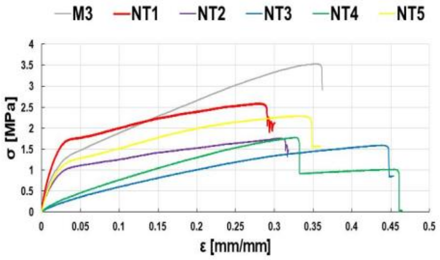

Figure 58. The σ/ε curves for NT materials and the comparison of the average behaviours with the average behaviour of M3

5.2.2. NF materials

Figure 62 shows the stress-strain curves for the tested specimens. The last image (bottom right) is a representation of the averages obtained for each material (these are marked with labels in all other representations), compared to the reference material (M3) and, it can be seen that the closest answer is that of the NF4 material.

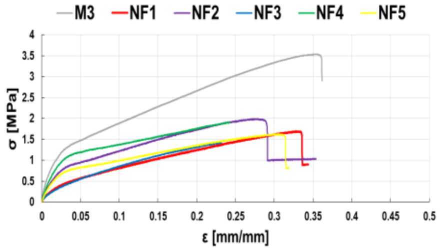

Figure 62. Stress-strain curves - NF materials

5.2.3. NE materials

Materials in this class have been formed in order to identify a possible effect of the application of a sinusoidal electric field on the formation of agglomerations of nanometric dimensions. From a mechanical point of view, it is expected that their response will be weak.

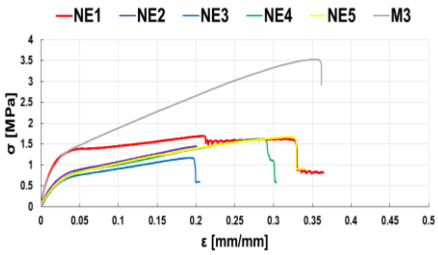

Figure 66. Stress-strain curves - NE materials

Analyzing all the results presented so far, it is very clear that the mechanical response of each material formed as a result of a special process is inferior to the response of the reference material - M3. This was expected as long as the presence of the PVP/NMP solution in the epoxy matrix is higher than the presence of the PVP/NMP solution in the epoxy matrix of the reference material. Chapter three analyzed the mechanical response of the reference materials and found that there is a direct causal relationship between the volume fraction of the PVP/NMP solution in the epoxy matrix and the mechanical response of the material.

5.2.4. Comparative analysis

Analyzing the data presented in Figure 70, it can be seen that the least effect on the mechanical response was the exposure to electromagnetic radiation. In this case, the mean curves indicate that the effect of maintaining exposure does not depend on the duration of exposure and the response is always lower than the response of the reference material. The NT1 material is the only one that, in the first part of the engagement, has a superior response to the M3 reference material but, once the treatment is maintained for a longer period, the response is weaker.

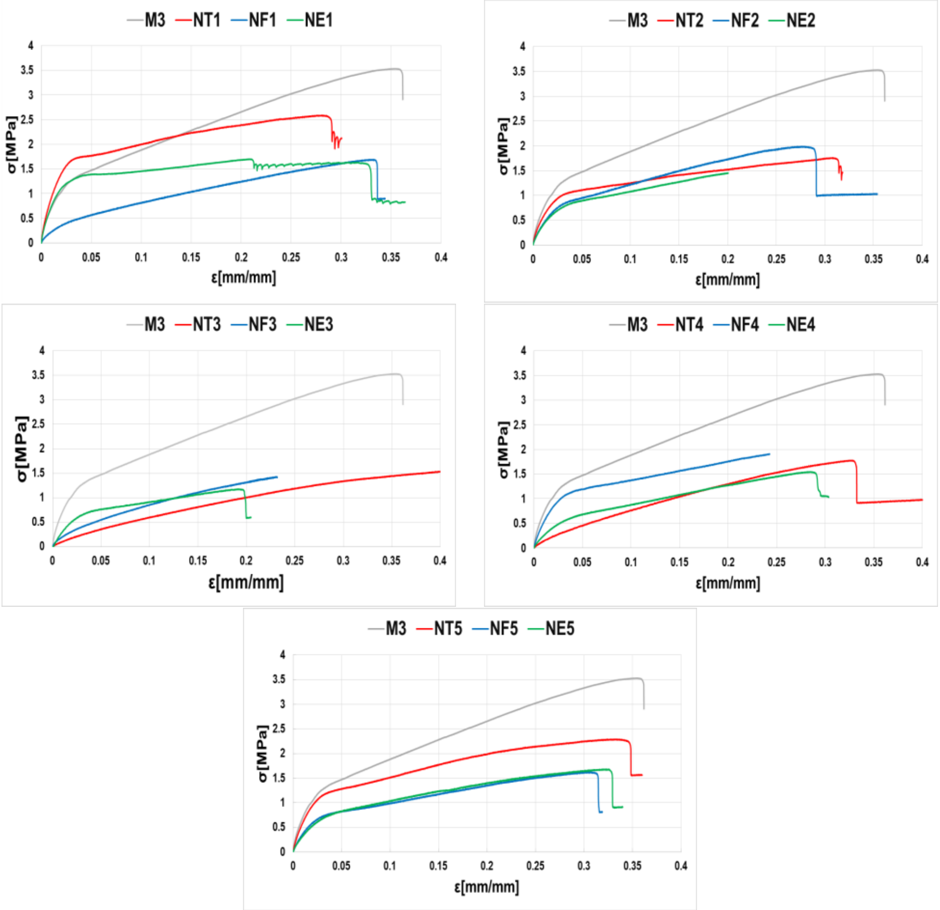

Figure 70. Average stress-strain curves for materials formed following additional treatments applied over the same period

Conclusions

- it is obvious that all the materials formed in this study have weaker mechanical responses than the response of the reference material - M3, but this can be explained by the increase of PVP/NMP concentration in the epoxy matrix;
- exposure to electromagnetic radiation and exposure to a sinusoidal electric field (over thermal exposure) aimed at quickly obtaining ceramic structures of nanometric dimensions and confirmation of this approach can not come from the mechanical analysis of materials (at least at the current level of technical development of instruments measurement).

5.3. Calorimetric analysis of N materials

For this analysis, in view of the results obtained from the analysis of the other materials (those presented in Chapters Three and Four) and the very large number of samples, the test method was modified to reduce - to some extent - the duration of each test and, implicitly the full duration of the data collection. The decision is also based on the fact that, as can be seen in Figures 5 (Chapter Three) and 22 (Chapter Four), the behaviour on the cooling segments for each material is the same.

Figure 79 shows the specific heat variation curves with temperature for equal periods of application of special treatments. The most important observation is that, apparently, after exposure to various treatments, for 96 hours, the materials obtained have identical thermal behaviour. If we refer to mechanical properties, we know that the materials have a very weak modulus of elasticity. The other observation was somewhat outlined in the first part of this analysis, namely that exposure to electromagnetic radiation changes the behaviour of materials too little (given that this exposure is superimposed on heat treatment). Thus, perhaps with the exception of materials treated for 48 hours, materials exposed to electromagnetic radiation have slightly higher values of specific heat compared to the specific heat values of NT materials.

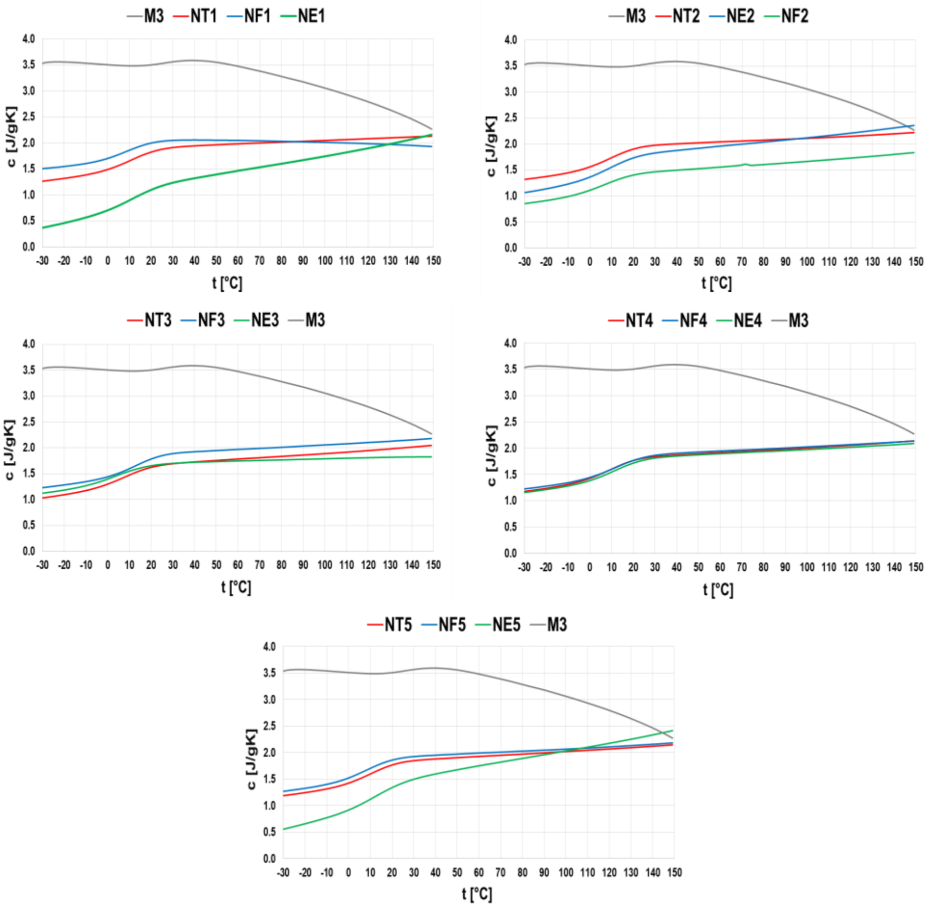

Figure 79. Specific heat variation curves with temperature - equal durations of treatments

Conclusions

- Apparently, exposure to electromagnetic radiation slightly increases the specific heat values of materials (compared to NT class materials). As the exposure to electromagnetic radiation (in the infrared and visible range - green-blue) is simultaneous with the heat treatment applied to all materials, it means that this exposure repairs, to some extent, the defects caused by permanent maintenance at a temperature of 70°C;
- the calorimetric analysis also shows that in order to maintain the treatments for 72 and 96 hours, respectively, changes occur with consequences on the properties of the formed materials. But why these changes are mitigated after maintaining the special conditions for 120 hours, remains an unanswered question;

5.4. Raman spectrophotometry of N materials

What is obvious is that type E materials (exposure to sinusoidal electric field) have the highest intensities of Raman signals (the exceptions are the already known case of maintaining special treatment for 48 hours, in which all materials give almost identical signals and the case of maintaining special conditions for 120 hours). The lowest intensity of the Raman signal is usually found for NF materials and could mean that due to electromagnetic irradiation (with radiation having the two wavelengths mentioned above) have somehow attenuated the vibration modes of the molecules that give signals in other cases (figure 82).

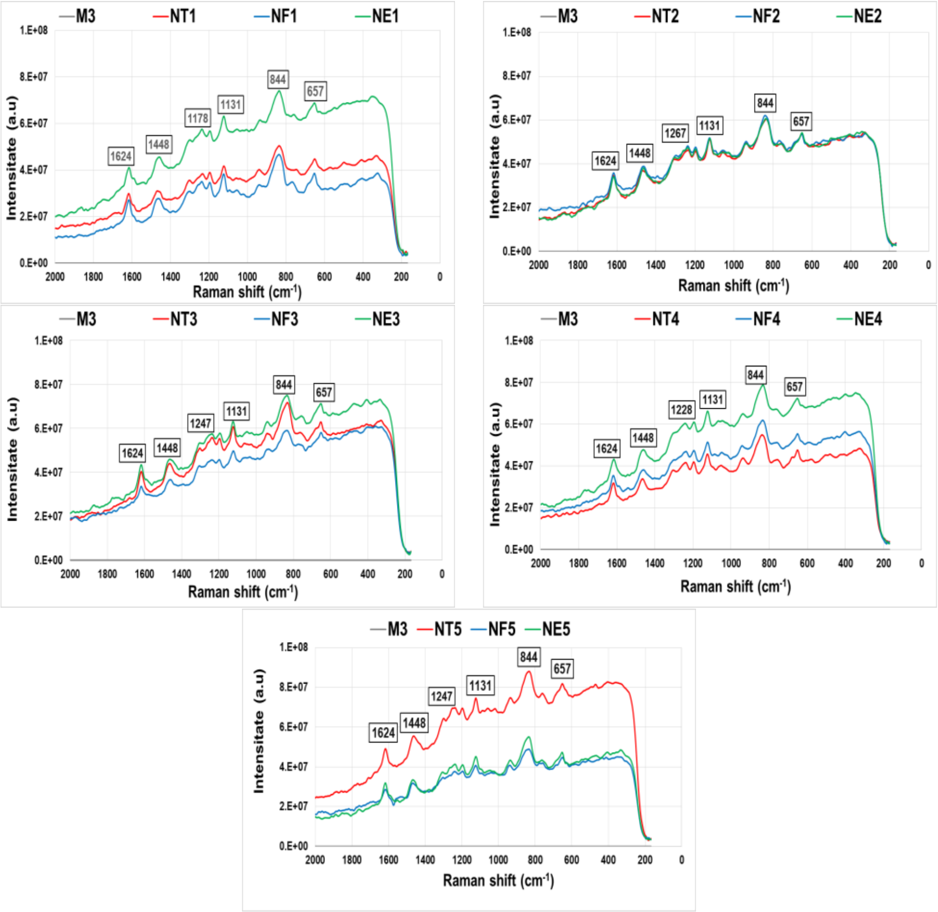

Figure 82. Raman spectra of materials depending on the duration of treatment

Conclusions

- in the case of mixtures prepared under special conditions, an alteration of the Raman signals may be observed for pre-NF mixtures with long durations for maintaining the special conditions (72, 96 and 120 hours), mixtures exposed for short periods (24 and 48 hours) practically do not give Raman signal;
- in the case of materials subjected to the thermal regime, the most intense signals are those given to the less exposed mixtures (24 and 48 hours);

- there is uniformity in the intensities of the Raman signals of the materials (after polymerisation) formed after maintaining the special conditions for 48 hours;

5.5. SEM analysis of N materials

5.5.1. NT materials

The SEM analysis was performed on samples exposed to special forming conditions for durations of 48, 72 and 96 hours, respectively. Figure 83 shows images of NT materials. It should be mentioned, from the very beginning, that a sample (from 15 formats) was chosen at random. This sample was broken (cooling was done with liquid nitrogen) to highlight a fracturing surface on which to investigate. Therefore, everything is statistical and the interpretation of the results must also be statistical. The above images are not a rule for NT materials.

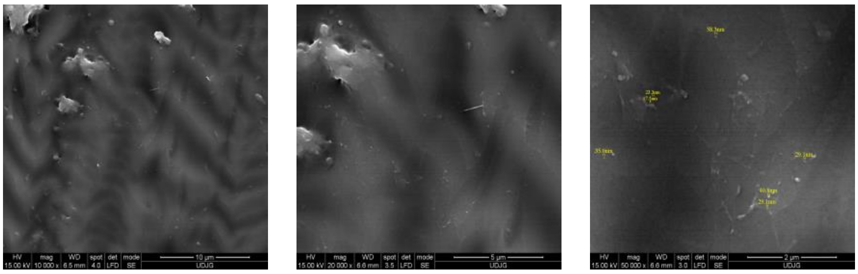

SEM images NT2

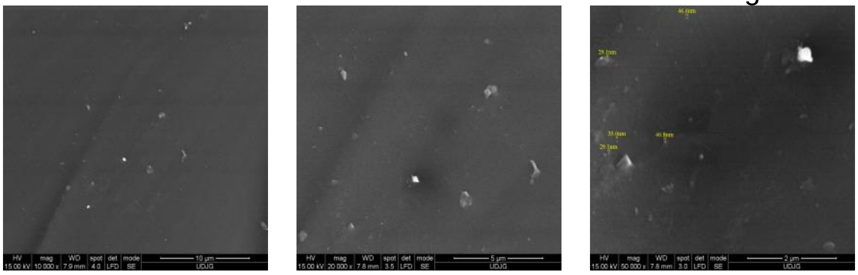

SEM images NT3

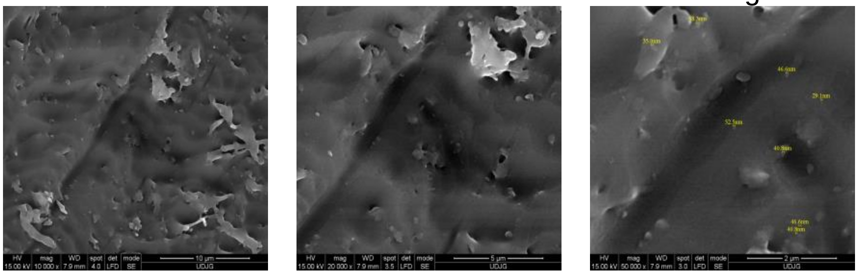

SEM images NT4

Figure 83. SEM analysis of NT materials

5.5.2. NF materials

NF materials are materials formed by applying additional exposure to electromagnetic radiation (with two wavelengths - one in the infrared range and one in the visible range, green-blue). SEM images indicate morphological changes due to the duration of special treatment. Apparently, there is a higher density of formations but nanometric dimensions in cases where the duration of exposure to special conditions is longer. What is interesting, although the probability is low, is that the general morphology of the investigated area is different depending on the duration of exposure. However, it is a matter of probability to choose the areas of investigation and, in these circumstances, any categorical statement is risky.

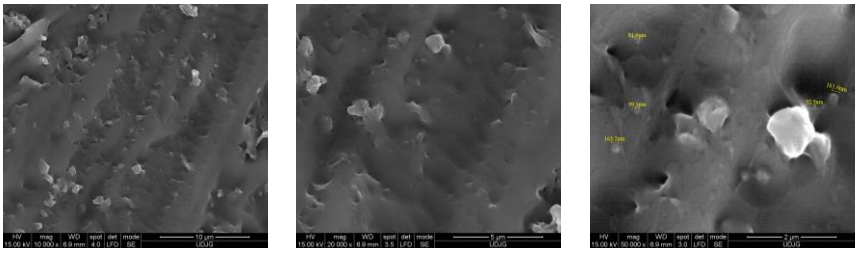

SEM images NF2

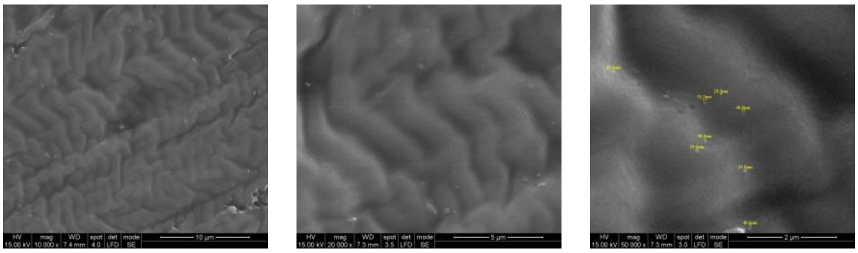

SEM images NF3

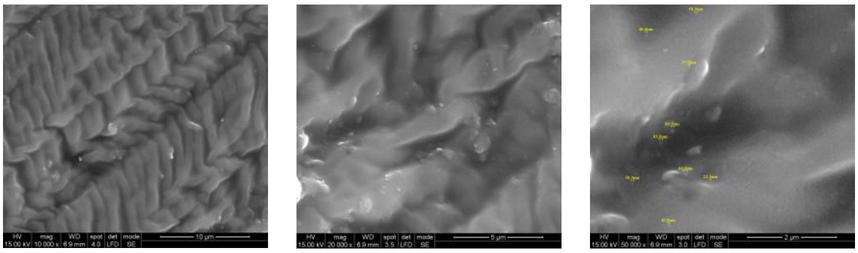

SEM images NF4

Figure 84. SEM analysis of NF materials

5.5.3. NE materials

Analyzing only the data in the right column, it could be concluded that a shorter exposure (to sinusoidal electric field) leads to a higher density of structures with nanometric dimensions.

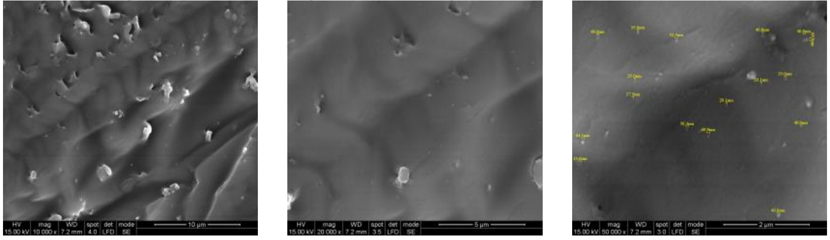

SEM images NE2

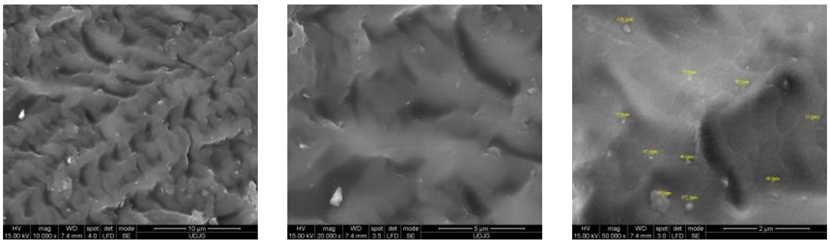

SEM images NE3

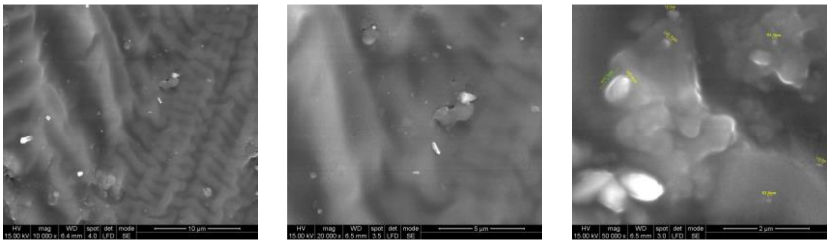

SEM images NE4

Figure 85. SEM analysis of NE materials

Conclusions

- there is insufficient information to be able to draw a conclusion on the effect of the treatments or the effect of maintaining the treatments for different durations;
- this analysis is practically insufficient without the informational support of the EDX analysis (which could not be performed at the time of the SEM analyzes).

5.6. EDX analysis of N materials

Regarding how the investigation was carried out, it should be noted that, on the fracture surfaces, areas of interest and points of interest were first searched, respectively (of interest means those areas or points where structures can be observed after an SEM analysis, necessary in the context of performing EDX). In a way, an analysis protocol was created that would allow an easy comparison of the results obtained (same magnifications, same elements followed) so that the results can be easily compared.

5.6.4. Intermaterial analysis - 48 hours of special treatment

In figure 95 it can be seen that the abundances of yttrium are lower for NE type materials, compared to the other two types of materials.

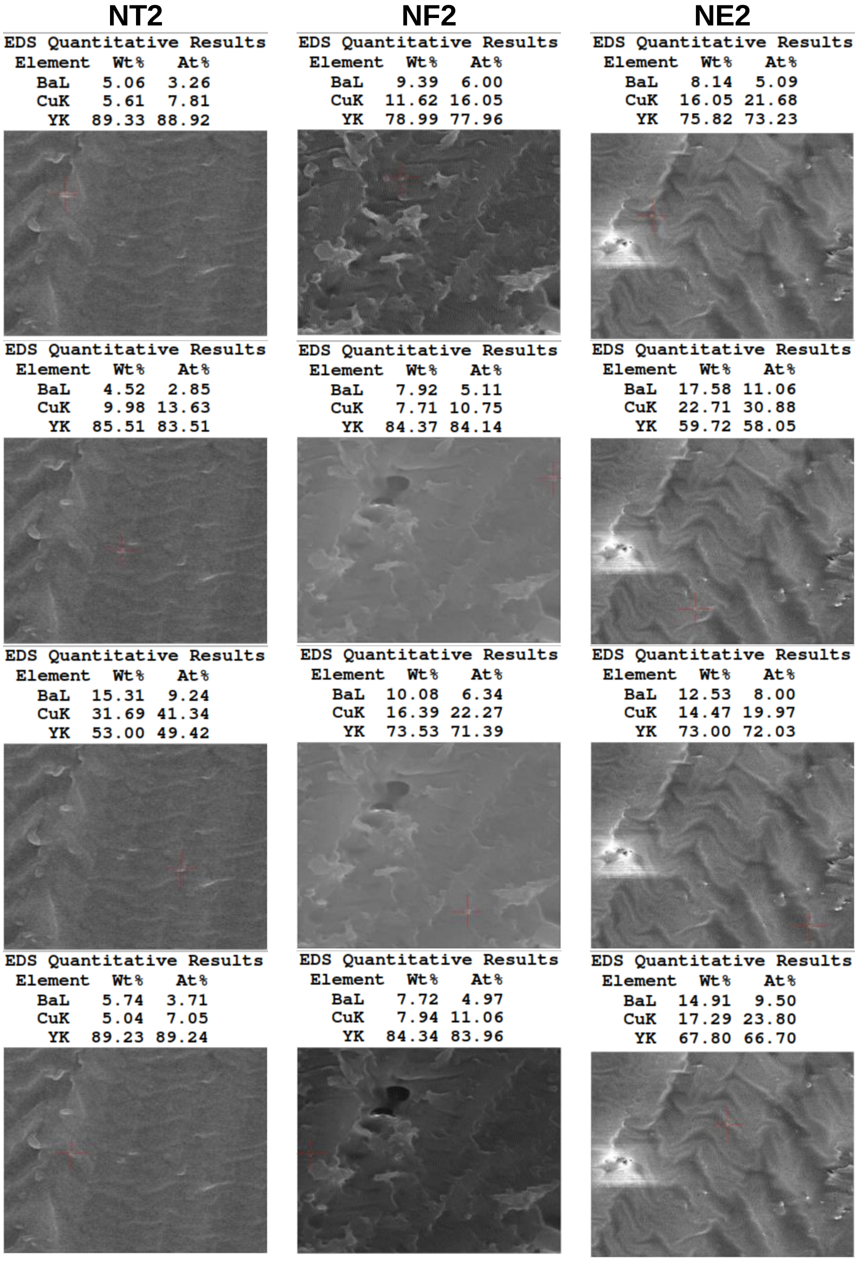

```
          NT2                           NF2                           NE2
EDS Quantitative Results      EDS Quantitative Results      EDS Quantitative Results
 Element  Wt%   At%            Element  Wt%   At%            Element  Wt%   At%
   BaL    5.06  3.26             BaL    9.39  6.00             BaL    8.14  5.09
   CuK    5.61  7.81             CuK   11.62 16.05             CuK   16.05 21.68
    YK   89.33 88.92              YK   78.99 77.96              YK   75.82 73.23

EDS Quantitative Results      EDS Quantitative Results      EDS Quantitative Results
 Element  Wt%   At%            Element  Wt%   At%            Element  Wt%   At%
   BaL    4.52  2.85             BaL    7.92  5.11             BaL   17.58 11.06
   CuK    9.98 13.63             CuK    7.71 10.75             CuK   22.71 30.88
    YK   85.51 83.51              YK   84.37 84.14              YK   59.72 58.05

EDS Quantitative Results      EDS Quantitative Results      EDS Quantitative Results
 Element  Wt%   At%            Element  Wt%   At%            Element  Wt%   At%
   BaL   15.31  9.24             BaL   10.08  6.34             BaL   12.53  8.00
   CuK   31.69 41.34             CuK   16.39 22.27             CuK   14.47 19.97
    YK   53.00 49.42              YK   73.53 71.39              YK   73.00 72.03

EDS Quantitative Results      EDS Quantitative Results      EDS Quantitative Results
 Element  Wt%   At%            Element  Wt%   At%            Element  Wt%   At%
   BaL    5.74  3.71             BaL    7.72  4.97             BaL   14.91  9.50
   CuK    5.04  7.05             CuK    7.94 11.06             CuK   17.29 23.80
    YK   89.23 89.24              YK   84.34 83.96              YK   67.80 66.70
```

Figure 15. Punctual elemental analyzes for materials exposed to special treatments for 48 hours

5.6.5. Intermaterial analysis - 72 hours of special treatment

For the materials subjected to special treatments for 72 hours, the results of the punctual elemental analyzes are presented in figure 97. The abundances of the three metals in different points (chosen at random) have dispersed values. Only for the second point of the NE3 material, a certain proportionality of the values of the abundances of the three metals can be observed, suggesting a structure.

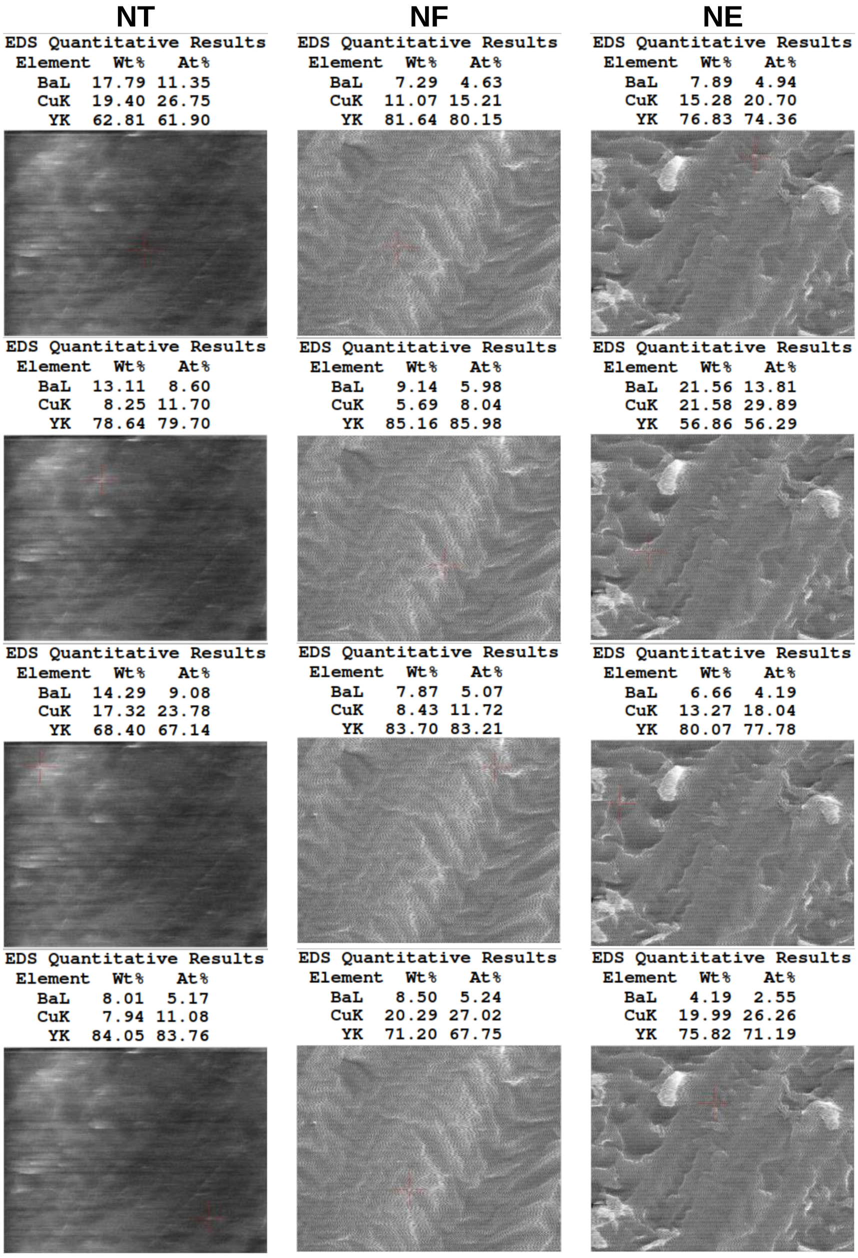

EDS Quantitative Results

Element	Wt%	At%
BaL	17.79	11.35
CuK	19.40	26.75
YK	62.81	61.90

EDS Quantitative Results

Element	Wt%	At%
BaL	7.29	4.63
CuK	11.07	15.21
YK	81.64	80.15

EDS Quantitative Results

Element	Wt%	At%
BaL	7.89	4.94
CuK	15.28	20.70
YK	76.83	74.36

EDS Quantitative Results

Element	Wt%	At%
BaL	13.11	8.60
CuK	8.25	11.70
YK	78.64	79.70

EDS Quantitative Results

Element	Wt%	At%
BaL	9.14	5.98
CuK	5.69	8.04
YK	85.16	85.98

EDS Quantitative Results

Element	Wt%	At%
BaL	21.56	13.81
CuK	21.58	29.89
YK	56.86	56.29

EDS Quantitative Results

Element	Wt%	At%
BaL	14.29	9.08
CuK	17.32	23.78
YK	68.40	67.14

EDS Quantitative Results

Element	Wt%	At%
BaL	7.87	5.07
CuK	8.43	11.72
YK	83.70	83.21

EDS Quantitative Results

Element	Wt%	At%
BaL	6.66	4.19
CuK	13.27	18.04
YK	80.07	77.78

EDS Quantitative Results

Element	Wt%	At%
BaL	8.01	5.17
CuK	7.94	11.08
YK	84.05	83.76

EDS Quantitative Results

Element	Wt%	At%
BaL	8.50	5.24
CuK	20.29	27.02
YK	71.20	67.75

EDS Quantitative Results

Element	Wt%	At%
BaL	4.19	2.55
CuK	19.99	26.26
YK	75.82	71.19

Figure 97. Punctual elemental analyzes for materials exposed to special treatments for 72 hours

5.6.6. Intermaterial analysis - 96 hours of special treatment

It is very difficult to specify, strictly following the distribution maps of the three elements if at certain points there are all three. This is the reason why, in figure 102, the superimposed maps of the three metals are represented, on the one hand, and, on the other hand, the map of the three elements superimposed on the SEM image of the analyzed area.

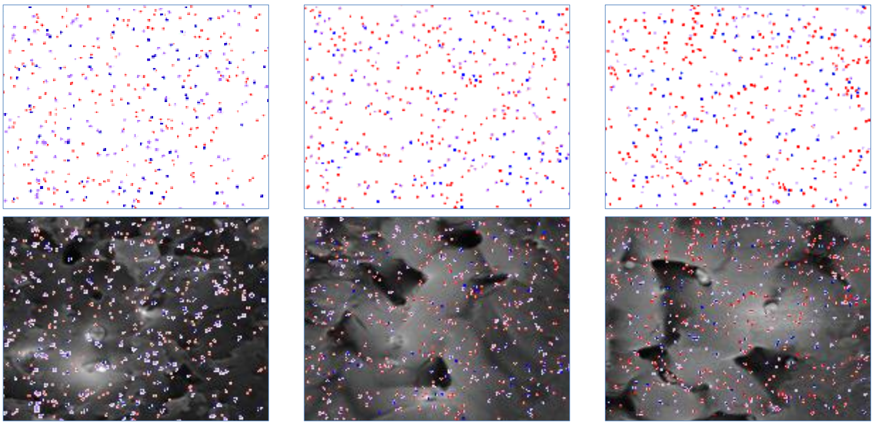

NT4 – 120µm^2 **NF4 – 120µm^2** **NE4 – 120µm^2**

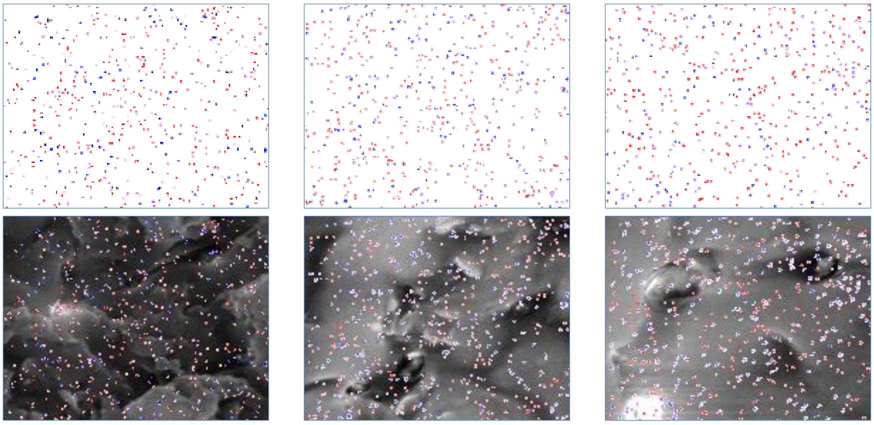

NT4 – 60µm^2 **NF4 – 60µm^2** **NE4 – 60µm^2**

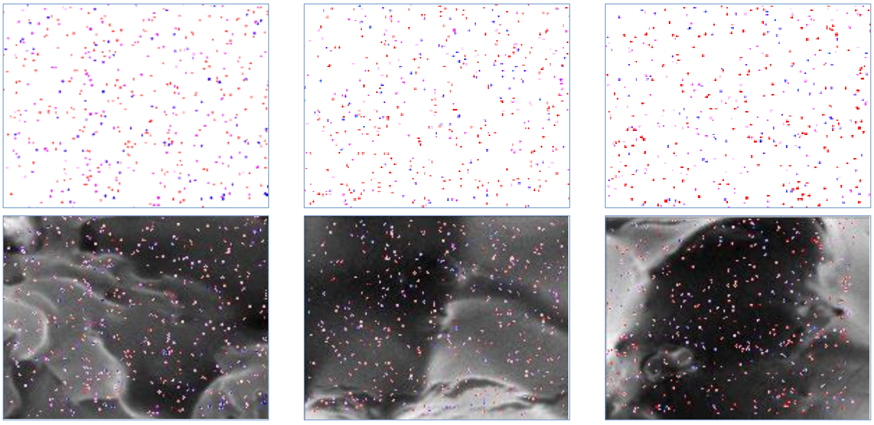

NT4 – 25µm^2 **NF4 – 25µm^2** **NE4 – 25µm^2**

Figure 102. Distributions of elements superimposed on SEM images

Conclusions

- both metal distribution maps and metal abundance were analyzed at some points of interest, but it is not possible to determine whether or not nanostructures exist;
- although more than 200 analyzes have been performed, the results cannot be interpreted correctly without the introduction of an analysis algorithm that would allow each element to be prioritized;
- overlapping distribution maps of the three metals were made and they allow the observation of the presence of all three species investigated in some points of the polymer matrix.

6. Conclusions and future studies

As stated in the presentation, this study was designed to test a hypothesis - the possibility of obtaining ceramic structures of nanometric size by developing possible reactions directly in the volume of epoxy resin.

It is certain that in the method of gels (citrate or oxalic) the combustion of the gel contributes to the *resetting* of the reactants (yttrium, barium and copper salts) - at energy level but the whole gel aims to reduce the reaction possibilities of the reactants (favouring local reactions). In the case of the present study, the viscosity of the resin should ensure the localization of the chemical reactions and the fact that the polymerization reaction is slightly exoenergetic, could provide the energy necessary for the reset in structures of nanometric dimensions.

Two major objectives have been proposed, on the one hand, to test the hypothesis of the formation of nanostructures starting from metal salts and, on the other hand, to investigate the conditions under which the development of these nanostructures could be stimulated using external factors.

In the first stage, the solubility of salts in solvent (NMP) was tested, given that the effect of the presence of NMP in epoxy resin was known (a previous study initiated and conducted at CCDCOMT) and for the present study nitrates and chlorides of yttrium, barium, copper, silver and zirconium metals were tested.

- chlorides are either sparingly soluble or insoluble in NMP while nitrates (and zirconium oxynitrate) are more soluble;
- some solutions were obtained by keeping the mixture in a state of agitation (on a magnetic mixer) and at a relatively high temperature. Precipitates were observed when these conditions were removed. Under these conditions all solutions were maintained in special conditions;
- amounts of PVP (soluble in NMP) were used to stabilize the solutions, which increase the viscosity of the inorganic compounds in the solution by increasing the viscosity.

• the effect of adding PVP or another thermoplastic polymer soluble in NMP in the common solution of all inorganic agents should be studied in the future;
• it would be interesting to use polysulfone (which was also used in the above-mentioned study - Georgel Mihu) but also other thermoplastic polymers (ABS, PMMA, Elastolan - also studied by Georgel Mihu in a postdoctoral study not only with NMP but also with N, N dimethylformamide and 1.4 dioxane).

The idea of using PVP to stabilize solutions has led to the need to investigate the effect of the presence of PVP/NMP solution on the volume of epoxy resin. In this way, the need arose for the formation and characterization of the materials presented in Chapter Three (although the formation and testing were subsequent to the formation of modified materials with inorganic agent solutions in PVP/NMP).

- although the effects of the NMP presence in the resin volume on the mechanical properties of the epoxy resin (and even those of a polysulfone solution in NMP) were known, the study indicated that a 5% presence of PVP/NMP solution in the epoxy matrix reduces the modulus of elasticity value but retains the appearance of rigid breaking of the material;
- at higher concentrations (10% and 15%) the materials show a viscoelastic behaviour (after testing the materials return to their original shape and dimensions even in the grip area). The broken samples also returned to their original shape so that the areas where the necks were produced (similar to thermoplastic polymers) can no longer be observed;

• in this context, it would be interesting to study the use of these materials instead of elastomers.

- mass losses (recorded during calorimetric analyzes) indicate their dependence on the share of the presence of PVP/NMP solution in the epoxy matrix;
- the source of the mass loss cannot be specified (boiling point values of NMP and PVP are higher than the maximum temperature reached during the test);
- there is a shift towards lower temperatures of the glass transition point of the epoxy resin as the weight of PVP/NMP in the matrix increases;
- thermomechanical analysis - aiming to determine the coefficient of linear thermal expansion of materials (considered homogeneous and isotropic for this type of analysis) - indicates that the dimensional stability of materials decreases with increasing weight of PVP/NMP in the epoxy

matrix;

- Raman analysis does not give indications on the properties of materials mainly because the PVP/NMP solution in the epoxy matrix does not have a high enough concentration to provide significant Raman signals.

For the materials modified with solutions of inorganic agents in PVP/NMP, metal nitrates were chosen (except for zirconium for which hydrate oxynitrate was used). The study was to answer the question of whether it is possible to obtain ceramic structures with nanometric dimensions.

- two strategies have been established, one in which the separate solutions of the inorganic agents are mixed and the mixture is placed in the epoxy resin (*global* strategy) and one strategy in which the PVP/NMP solution of each inorganic agent is placed in the resin and then these mixtures are mixed and homogenized together (*separately* strategy);
- for each of the two strategies, materials were formed that respect the PVP/NMP concentrations in the case of the materials presented in Chapter Three (unfortunately the materials with the highest concentration have disappeared ...);
- the results of the mechanical tests suggest the formation of weaker materials (compared to the reference materials - M1 and M2) but these results may be strongly influenced by the presence of water (enemy of epoxy resin) introduced into the system with hydrated salts;
- the presence of water leads to the cancellation of some bonds made by polymerization and, on the other hand, there is a possibility that the ions from the solubilization of the salts also block some possibility of binding of the resin molecules;

• it would be interesting to study the effect of inorganic agents taken separately because the influences of both water (hydration) and ions could be highlighted. One such study could complement another, designed and conducted at CCDCOMT, on the doping of epoxy resins with metal ions (Iulia Păduraru-Graur);

• also in this sense, it would be interesting a study to follow the method proposed by the aforementioned study - solvation of salts in slightly volatile organic solvents to be removed after mixing with epoxy resin.

- the results of the calorimetric tests are in line with the observations made for the epoxy resins modified with PVP/NMP solution;
- the losses of substance are a bit higher and here an explanation could be the dehydration (ie the removal of the water introduced with the hydrated salts;
- the thermomechanical analysis leads to the conclusion that all materials modified with solutions of inorganic agents in PVP/NMP have a higher coefficient of linear thermal expansion than analogous materials modified with only PVP/NMP;
- Raman analysis cannot reveal the possible consequences of the presence of metals - especially since they are in very low concentration in the epoxy matrix;

• due to the fact that the concentration of metals cannot be increased (under the conditions of the present study) this increase may be possible by increasing the concentration of the PVP/NMP solution or other thermoplastic polymer/NMP.

- the SEM analysis indicates that in the case of ZBAO not even agglomerations of metals are made and not so many structures while in the case of the other combination of metals certain structures are registered;
- the EDX analysis indicates that in the case of YBCO there are points where the three metals meet together;
- in the case of ZBAO, no more than two of the three metals are found in the same points, which leads to the conclusion that this combination cannot lead to the formation of nanostructures;
- the separate strategy did not lead to notable results (for either of the two proposed combinations) probably also due to the very low concentration of inorganic agents;
- in the case of YBCO, the overall strategy resulted in a higher concentration of inorganic compounds, which is why it was adopted for further study.

The second major objective was to identify ways to stimulate the development of local chemical reactions.

- a first approach was to maintain the solution of the inorganic agents in PVP/NMP for a longer time under stirring conditions (magnetic stirrer) at a temperature of 70°C;
- a second approach was to expose the solution of inorganic agents in PVP/NMP - at the same time as maintaining a state of agitation to a temperature of 70°C - to the action of electromagnetic

radiation (a wavelength in IR and a visible wavelength);

- the third approach - together with maintaining the conditions defined in the first approach - exposure, for 30 minutes, every 24 hours, to the action of a sinusoidal electric field of 30kHz frequency;
- the materials formed were obtained after maintaining the special conditions for 24, 48, 72, 96 and 120 hours respectively, provided that the mixture of the inorganic agent solution in PVP/NMP had been homogenized before for 168 hours;
- the materials obtained have a PVP/NMP solution concentration of 18,5% higher than the materials analyzed in Chapter Three and, consequently, their mechanical properties were expected to be lower than any of them, in this case, M3 with a concentration of 15%;
- it is obvious that all the materials formed in this study have weaker mechanical responses than the response of the reference material - M3, but this can be explained by the increase of PVP/NMP concentration in the epoxy matrix;
- within the limits of measurement errors, in some cases, the previous statement is not valid, suggesting important changes induced by special treatments (electromagnetic exposure, exposure to the sinusoidal electric field);
- apparently, some special treatments repair the effects induced by the main (thermal) treatment but the experimental data are not sufficient for such a conclusion;
- there are insufficient data - mainly due to experimental errors - to conclude decisively on the effect of the application of the special treatment on the mechanical properties of the formed materials;
- apparently, the heat treatment (that applied to all mixtures) is destructive in terms of the mechanical response of the materials and this can be explained by blocking the formation of bonds leading to the formation of polymer networks due to thermal agitation and the presence of inorganic agents;
- in view of maintaining the mixtures at high temperatures, it is possible to vaporize some organic components; in this case, the disappearance of some organic compounds would affect the final properties of the materials;
- exposure to electromagnetic radiation and exposure to sinusoidal electric field (over thermal exposure) aimed at quickly obtaining ceramic structures of nanometric dimensions and confirmation of this approach can not come from the mechanical analysis of materials (at least at the current level of technical development of instruments measurement);
- these conditions would be interesting to study, in which the special conditions are maintained for shorter periods (taking into account the results obtained for material B(g)6, presented in the fourth chapter);
- the two wavelengths of electromagnetic radiation were used - one to heat the mixture (the IR) and one to stabilize the copper compounds (the visible);
- under these conditions a study of the dependence of the properties of epoxy resin and epoxy resin modified with solutions of inorganic agents in thermoplastic polymer / NMP solutions on the wavelength of electromagnetic radiation maintained during sample preparation and polymerization could be initiated.
- given that the viscosity of the resin is high enough, it can be assumed that the mobility of the various ion species is very low so that the application of a sinusoidal electric field could only lead to a possible destabilization of them favouring the achievement of connections;
- the application of special treatments during the preparation of the materials leads to the decrease of the specific heat values;
- Apparently, exposure to electromagnetic radiation slightly increases the specific heat values of materials (compared to NT class materials). As the exposure to electromagnetic radiation (in the infrared and visible range - green-blue) is simultaneous with the heat treatment applied to all materials means that this exposure repairs, to some extent, the defects caused by the permanent maintenance of a temperature of 70°C;
- exposure to a sinusoidal electric field appears to cause the greatest damage, in the sense that the materials thus obtained have the lowest values of specific heat in the field of low-temperature values;
- the analysis of substance losses during the tests shows that all materials in class N have lower mass losses than the losses of the reference material, although the volume fraction of the PVP/NMP solution is higher in N materials (18.75%) than in reference - M3 (15%). This could

mean that most of the volatile components in the mixture are lost during heat treatment - the mass losses are approximately equal for all materials analyzed;
- in the case of mixtures prepared under special conditions, an alteration of the Raman signals may be observed for pre-NF mixtures with long durations for maintaining the special conditions (72, 96 and 120 hours), mixtures exposed for short periods (24 and 48 hours) do not give, partially, Raman signal;
- in the case of materials subjected to the thermal regime, the most intense signals are those given to the less exposed mixtures (24 and 48 hours);
- the only mixtures that give signals (with different intensities) are those that have been exposed to the sinusoidal electric field and there does not seem to be a link between the signal intensity and the duration of exposure to special conditions;
- there is uniformity in the intensities of the Raman signals of the materials (after polymerisation) formed after maintaining the special conditions for 48 hours;
- for the longest duration of exposure to special conditions the most intense signal is given by the NT material (and is also more intense than the signal corresponding to the minimum duration of exposure);
- in general, the weakest signal is that of NF materials and the signal strength depends very little on the duration of maintaining the special conditions;
- both metal distribution maps and metal abundance were analyzed at some points of interest, but it is not possible to determine whether or not nanostructures exist;
- although more than 200 analyzes have been performed, the results cannot be interpreted correctly without the introduction of an analysis algorithm that would allow each element to be prioritized;
- overlapping distribution maps of the three metals were made and they allow the observation of the presence of all three species investigated in some points of the polymer matrix.

Bibliografy

[1] M. C. García and F. Quiroz, “Nanostructured polymers,” in *Nanobiomaterials*, Elsevier, 2018, pp. 339–356.

[2] L. Peponi, D. Puglia, L. Torre, L. Valentini, and J. M. Kenny, “Processing of nanostructured polymers and advanced polymeric based nanocomposites,” *Materials Science and Engineering: R: Reports*, vol. 85, pp. 1–46, Nov. 2014, doi: 10.1016/j.mser.2014.08.002.

[3] U. Wiesner, “Hybrid Polymer–Inorganic Nanostructures,” in *Polymer Science: A Comprehensive Reference*, Elsevier, 2012, pp. 129–140.

[4] A. B. Reddy, G. S. M. Reddy, V. Sivanjineyulu, J. Jayaramudu, K. Varaprasad, and E. R. Sadiku, “Hydrophobic/Hydrophilic Nanostructured Polymer Blends,” in *Design and Applications of Nanostructured Polymer Blends and Nanocomposite Systems*, Elsevier, 2016, pp. 385–411.

[5] S. H. Whang, Ed., *Nanostructured metals and alloys: processing, microstructure, mechanical properties and applications*. Oxford: WP, Woodhead Publ, 2011.

[6] Z. Tang *et al.*, “Polymeric nanostructured materials for biomedical applications,” *Progress in Polymer Science*, vol. 60, pp. 86–128, Sep. 2016, doi: 10.1016/j.progpolymsci.2016.05.005.

[7] A. Adeniyi *et al.*, “Thermoplastic-Thermoset Nanostructured Polymer Blends,” in *Design and Applications of Nanostructured Polymer Blends and Nanocomposite Systems*, Elsevier, 2016, pp. 15–38.

[8] E. R. Sadiku *et al.*, “Nanostructured Polymer Blends for Gas/Vapor Barrier and Dielectric Applications,” in *Design and Applications of Nanostructured Polymer Blends and Nanocomposite Systems*, Elsevier, 2016, pp. 239–259.

[9] A. Lu and R. K. O’Reilly, “Advances in nanoreactor technology using polymeric nanostructures,” *Current Opinion in Biotechnology*, vol. 24, no. 4, pp. 639–645, Aug. 2013, doi: 10.1016/j.copbio.2012.11.013.

[10] S. Zavyalov, “Formation and characterization of metal-polymer nanostructured composites,” *Solid State Ionics*, vol. 147, no. 3–4, pp. 415–419, Apr. 2002, doi: 10.1016/S0167-2738(02)00038-3.

[11] S. Thomas, A. P. Mathew, and V. P. M., Eds., *Advances in natural polymers: composites and nanocomposites*. Heidelberg ; New York: Springer, 2013.

[12] E. M. Pearce, B. A. Howell, R. A. Pethrick, and G. E. Zaikov, Eds., *Physical chemistry research for engineering and applied sciences*. Oakville, ON, Canada ; Waretown, NJ, USA: Apple Academic Press, 2015.

[13] B. J. Briscoe and S. K. Sinha, “Tribological applications of polymers and their composites – past, present and future prospects,” in *Tribology of Polymeric Nanocomposites*, Elsevier, 2013, pp. 1–22.

[14] H. C. Guo, E. Ye, Z. Li, M.-Y. Han, and X. J. Loh, “Recent progress of atomic layer deposition on polymeric materials,” *Materials Science and Engineering: C*, vol. 70, pp. 1182–1191, Jan. 2017, doi: 10.1016/j.msec.2016.01.093.

[15] L. McKeen, “Introduction to Plastics and Polymers,” in *The Effect of Sterilization Methods on Plastics and Elastomers*, Elsevier, 2018, pp. 41–61.

[16] J. R. Fried, *Polymer science and technology*, Third edition. Upper Saddle River, NJ: Prentice Hall, 2014.

[17] M. Buggy, “Polymeric Materials,” in *Reference Module in Materials Science and Materials Engineering*, Elsevier, 2016.

[18] R. J. Young and P. A. Lovell, *Introduction to polymers*. Boca Raton: CRC Press, 2011.

[19] F. Cravero, S. A. Schustik, M. J. Martínez, C. D. Barranco, M. F. Díaz, and I. Ponzoni, “Computer-aided design of polymeric materials: Computational study for characterization of databases for prediction of mechanical properties under polydispersity,” *Chemometrics and*

Intelligent Laboratory Systems, vol. 191, pp. 65–72, Aug. 2019, doi: 10.1016/j.chemolab.2019.06.006.

[20] G. G. Odian, *Principles of polymerization*, 4th ed. Hoboken, N.J: Wiley-Interscience, 2004.

[21] C. I. Awuzie, “Conducting Polymers,” *Materials Today: Proceedings*, vol. 4, no. 4, pp. 5721–5726, 2017, doi: 10.1016/j.matpr.2017.06.036.

[22] Y. Weitsman, *Fluid effects in polymers and polymeric composites*. New York: Springer, 2012.

[23] S. Chikkali, Ed., *Metal-catalyzed polymerization: fundamentals to applications*. Boca Raton: CRC Press, 2018.

[24] *Design and applications of nanostructured polymer blends and nanocomposite systems*, 1st edition. Waltham, MA: Elsevier, 2015.

[25] V. Hasirci, P. Y. Huri, T. E. Tanir, G. Eke, and N. Hasirci, “1.22 Polymer Fundamentals: Polymer Synthesis ☆,” in *Comprehensive Biomaterials II*, Elsevier, 2017, pp. 478–506.

[26] E. Ojogbo, E. O. Ogunsona, and T. H. Mekonnen, “Chemical and physical modifications of starch for renewable polymeric materials,” *Materials Today Sustainability*, vol. 7–8, p. 100028, Mar. 2020, doi: 10.1016/j.mtsust.2019.100028.

[27] C. S. Brazel, S. L. Rosen, and S. L. Rosen, *Fundamental principles of polymeric materials*, Third edition. Hoboken, New Jersey: Wiley, 2012.

[28] H. Burhan, S. Saygili, and F. Şen, “Principal and mechanism of self-repair of polymer matrix composite materials,” in *Self-Healing Composite Materials*, Elsevier, 2020, pp. 193–208.

[29] M. S. Kondratenko, I. V. Elmanovich, and M. O. Gallyamov, “Polymer materials for electrochemical applications: Processing in supercritical fluids,” *The Journal of Supercritical Fluids*, vol. 127, pp. 229–246, Sep. 2017, doi: 10.1016/j.supflu.2017.03.011.

[30] T. Biswal, S. K. BadJena, and D. Pradhan, “Synthesis of polymer composite materials and their biomedical applications,” *Materials Today: Proceedings*, p. S2214785320306775, Feb. 2020, doi: 10.1016/j.matpr.2020.01.567.

[31] D. Banoriya, R. Purohit, and R. K. Dwivedi, “Advanced Application of Polymer based Biomaterials,” *Materials Today: Proceedings*, vol. 4, no. 2, pp. 3534–3541, 2017, doi: 10.1016/j.matpr.2017.02.244.

[32] B. A. Howell and American Chemical Society, Eds., *Introduction of macromolecular science/polymeric materials into the foundational course in organic chemistry*. Washington, DC: American Chemical Soc, 2013.

[33] R. Francis and D. S. Kumar, Eds., *Biomedical applications of polymeric materials and composites*. Weinheim: Wiley-VCH Verlag GmbH & Co. KGaA, 2017.

[34] H. R. Rezaie, A. Shokuhfar, and F. Arianpour, “Nanocomposite Materials from Theory to Application,” in *New Frontiers of Nanoparticles and Nanocomposite Materials*, vol. 4, A. Öchsner and A. Shokuhfar, Eds. Berlin, Heidelberg: Springer Berlin Heidelberg, 2012, pp. 171–232.

[35] R. O. Ebewele, *Polymer science and technology*. Boca Raton: CRC Press, 2000.

[36] N. Pande, N. P. S. Chauhan, D. Pande-Shrama, and M. Mozafari, “Conjugated polymers having semiconducting properties,” in *Advanced Functional Polymers for Biomedical Applications*, Elsevier, 2019, pp. 65–82.

[37] B. ter Horst, N. S. Moiemen, and L. M. Grover, “Natural polymers,” in *Biomaterials for Skin Repair and Regeneration*, Elsevier, 2019, pp. 151–192.

[38] B. M. Jarai, E. L. Kolewe, Z. S. Stillman, N. Raman, and C. A. Fromen, “Polymeric Nanoparticles,” in *Nanoparticles for Biomedical Applications*, Elsevier, 2020, pp. 303–324.

[39] L. Brunnbauer, S. Larisegger, H. Lohninger, M. Nelhiebel, and A. Limbeck, “Spatially resolved polymer classification using laser induced breakdown spectroscopy (LIBS) and multivariate statistics,” *Talanta*, vol. 209, p. 120572, Mar. 2020, doi: 10.1016/j.talanta.2019.120572.

[40] L. W. McKeen, “Introduction to Plastics and Polymers,” in *The Effect of UV Light and Weather on Plastics and Elastomers*, Elsevier, 2019, pp. 1–20.

[41] V. K. Thakur, M. K. Thakur, and M. R. Kessler, Eds., *Handbook of composites from renewable materials. Volume 1: Structure and chemistry*. Beverly, MA: Scrivener Publishing, 2017.

[42] Mohd. H. Othman, “Polymer Blends and Composites From Renewable Resources,” in *Encyclopedia of Renewable and Sustainable Materials*, Elsevier, 2020, pp. 179–186.

[43] C. Rauwendaal, *Polymer extrusion*, 5th edition. Munich : Cincinnati: Hanser Publications ; Hanser Publication, 2014.

[44] V. Di Noto, S. Lavina, G. A. Giffin, E. Negro, and B. Scrosati, “Polymer electrolytes: Present, past and future,” *Electrochimica Acta*, vol. 57, pp. 4–13, Dec. 2011, doi: 10.1016/j.electacta.2011.08.048.

[45] B. M. Mandal, *Fundamentals of polymerization*. Singapore: World Scientific, 2013.

[46] H. Zweifel, *Stabilization of Polymeric Materials*. Berlin, Heidelberg: Springer Berlin Heidelberg, 1998.

[47] I. Negut, V. Grumezescu, G. Dorcioman, and G. Socol, “Microscale Drug Delivery Systems: Current Perspectives and Novel Approaches,” in *Nano- and Microscale Drug Delivery Systems*, Elsevier, 2017, pp. 1–15.

[48] A. Shrivastava, “Polymerization,” in *Introduction to Plastics Engineering*, Elsevier, 2018, pp. 17–48.

[49] C.-S. Chern, *Principles and applications of emulsion polymerization*. Hoboken, N.J: Wiley, 2008.

[50] G. Moad, D. H. Solomon, and G. Moad, *The chemistry of radical polymerization*, 2nd fully rev. ed. Amsterdam ; Boston: Elsevier, 2006.

[51] A. B. Asha, S. Srinivas, X. Hao, and R. Narain, “Enzyme-Responsive Polymers: Classifications, Properties, Synthesis Strategies, and Applications,” in *Smart Polymers and their Applications*, Elsevier, 2019, pp. 155–189.

[52] S. Kobayashi and K. Müllen, Eds., *Encyclopedia of polymeric nanomaterials*. Berlin: Springer, 2015.

[53] Muralisrinivasan Subramanian, *Basics of polymers: fabrication and processing technology*. New York: Momentum Press., 2015.

[54] R. Das, *Polymeric materials for clean water*. 2019.

[55] S. Maji, V. V. Jerca, F. A. Jerca, and R. Hoogenboom, “Smart polymeric gels,” in *Polymeric Gels*, Elsevier, 2018, pp. 179–230.

[56] E. Saldívar-Guerra and E. Vivaldo-Lima, Eds., *Handbook of polymer synthesis, characterization, and processing*. Hoboken, New Jersey: Wiley, 2013.

[57] K. Kumar Patel and R. Purohit, “Future Prospects of shape memory polymer nano-composite and epoxy based shape memory polymer- A review,” *Materials Today: Proceedings*, vol. 5, no. 9, pp. 20193–20200, 2018, doi: 10.1016/j.matpr.2018.06.389.

[58] H. Münstedt, *Rheological and morphological properties of dispersed polymeric materials: filled polymers and polymer blends*. Munich : Cincinnati, Ohio: Hanser Publishers ; Hanser Publications, 2016.

[59] M. Niaounakis, “Compounding and Additives,” in *Biopolymers: Processing and Products*, Elsevier, 2015, pp. 215–262.

[60] D. C. González-Toro and S. Thayumanavan, “Advances in polymer and polymeric nanostructures for protein conjugation,” *European Polymer Journal*, vol. 49, no. 10, pp. 2906–2918, Oct. 2013, doi: 10.1016/j.eurpolymj.2013.05.002.

[61] A. A. Teran, M. H. Tang, S. A. Mullin, and N. P. Balsara, “Effect of molecular weight on conductivity of polymer electrolytes,” *Solid State Ionics*, vol. 203, no. 1, pp. 18–21, Nov. 2011, doi: 10.1016/j.ssi.2011.09.021.

[62] Ajitha A.R. and S. Thomas, “Introduction,” in *Compatibilization of Polymer Blends*, Elsevier, 2020, pp. 1–29.

[63] C. E. Estridge, “The effects of competitive primary and secondary amine reactivity on the structural evolution and properties of an epoxy thermoset resin during cure: A molecular dynamics study,” *Polymer*, vol. 141, pp. 12–20, Apr. 2018, doi: 10.1016/j.polymer.2018.02.062.

[64] Q. Yang, X. Li, L. Shi, X. Yang, and G. Sui, “The thermal characteristics of epoxy resin: Design and predict by using molecular simulation method,” *Polymer*, vol. 54, no. 23, pp. 6447–6454, Nov. 2013, doi: 10.1016/j.polymer.2013.09.055.

[65] F. Delor-Jestin, D. Drouin, P.-Y. Cheval, and J. Lacoste, “Thermal and photochemical ageing of epoxy resin – Influence of curing agents,” *Polymer Degradation and Stability*, vol. 91, no. 6, pp. 1247–1255, Jun. 2006, doi: 10.1016/j.polymdegradstab.2005.09.009.

[66] D. Ratna, *Handbook of thermoset resins*. Shawbury: iSmithers, 2009.

[67] Y.-J. Peng, X. He, Q. Wu, P.-C. Sun, C.-J. Wang, and X.-Z. Liu, “A new recyclable crosslinked polymer combined polyurethane and epoxy resin,” *Polymer*, vol. 149, pp. 154–163, Aug. 2018, doi: 10.1016/j.polymer.2018.06.082.

[68] J. Zhang *et al.*, “A bio-based hyperbranched flame retardant for epoxy resins,” *Chemical Engineering Journal*, vol. 381, p. 122719, Feb. 2020, doi: 10.1016/j.cej.2019.122719.

[69] S. C. Chowdhury, R. M. Elder, T. W. Sirk, and J. W. Gillespie, “Epoxy resin thermo-mechanics and failure modes: Effects of cure and cross-linker length,” *Composites Part B: Engineering*, vol. 186, p. 107814, Apr. 2020, doi: 10.1016/j.compositesb.2020.107814.

[70] S. Guo, Y. Lu, X. Wan, F. Wu, T. Zhao, and C. Shen, “Preparation, characterization of highly dispersed reduced graphene oxide/epoxy resin and its application in alkali-activated slag composites,” *Cement and Concrete Composites*, vol. 105, p. 103424, Jan. 2020, doi: 10.1016/j.cemconcomp.2019.103424.

[71] T. Vidil, F. Tournilhac, S. Musso, A. Robisson, and L. Leibler, “Control of reactions and network structures of epoxy thermosets,” *Progress in Polymer Science*, vol. 62, pp. 126–179, Nov. 2016, doi: 10.1016/j.progpolymsci.2016.06.003.

[72] M. Abd El-Rahman, K. M. Yassien, and A. A. M. Yassene, “Effect of gamma irradiation on the optical properties of epoxy resin thin films,” *Optik*, vol. 183, pp. 962–970, Apr. 2019, doi: 10.1016/j.ijleo.2018.12.182.

[73] M. Pecora, Y. Pannier, M.-C. Lafarie-Frenot, M. Gigliotti, and C. Guigon, “Effect of thermo-oxidation on the failure properties of an epoxy resin,” *Polymer Testing*, vol. 52, pp. 209–217, Jul. 2016, doi: 10.1016/j.polymertesting.2016.04.008.

[74] W. Ferdous, A. Manalo, T. Aravinthan, and G. Van Erp, “Properties of epoxy polymer concrete matrix: Effect of resin-to-filler ratio and determination of optimal mix for composite railway sleepers,” *Construction and Building Materials*, vol. 124, pp. 287–300, Oct. 2016, doi: 10.1016/j.conbuildmat.2016.07.111.

[75] G. H. Michler and F. J. Baltá-Calleja, *Nano- and micromechanics of polymers: structure modification and improvement of properties*. Cincinnati: Hanser Publications, 2012.

[76] J. Seo, N. Yui, and J.-H. Seo, “Development of a supramolecular accelerator simultaneously to increase the cross-linking density and ductility of an epoxy resin,” *Chemical Engineering Journal*, vol. 356, pp. 303–311, Jan. 2019, doi: 10.1016/j.cej.2018.09.020.

[77] I. A. Mohammed, M. F. Ali, and W. R. Wan Daud, “New class of liquid crystalline epoxy resins: Synthesis and properties,” *Journal of Industrial and Engineering Chemistry*, vol. 18, no. 1, pp. 364–372, Jan. 2012, doi: 10.1016/j.jiec.2011.11.100.

[78] K. S. Santhosh Kumar, R. Biju, and C. P. Reghunadhan Nair, “Progress in shape memory epoxy resins,” *Reactive and Functional Polymers*, vol. 73, no. 2, pp. 421–430, Feb. 2013, doi: 10.1016/j.reactfunctpolym.2012.06.009.

[79] M. Kubisztal, G. Haneczok, A. Chrobak, A. Kubik, and J. Rasek, “Study of epoxy resin curing process by applying internal friction technique,” *Materials Science and Engineering: A*, vol. 521–522, pp. 283–286, Sep. 2009, doi: 10.1016/j.msea.2008.09.127.

[80] M. Liang and K. L. Wong, "Study of Mechanical and Thermal Performances of Epoxy Resin Filled with Micro Particles and Nanoparticles," *Energy Procedia*, vol. 110, pp. 156–161, Mar. 2017, doi: 10.1016/j.egypro.2017.03.121.

[81] P. Yang, M. Ren, K. Chen, Y. Liang, Q.-F. Lü, and T. Zhang, "Synthesis of a novel silicon-containing epoxy resin and its effect on flame retardancy, thermal, and mechanical properties of thermosetting resins," *Materials Today Communications*, vol. 19, pp. 186–195, Jun. 2019, doi: 10.1016/j.mtcomm.2019.01.014.

[82] J. E. Figueruelo, C. M. Gómez, I. S. Monzó, C. Abad, and A. Campos, "Thermodynamic study on phase equilibrium of epoxy resin/thermoplastic blends," *The Journal of Chemical Thermodynamics*, vol. 40, no. 4, pp. 677–687, Apr. 2008, doi: 10.1016/j.jct.2007.10.009.

[83] C. A. May, Ed., *Epoxy resins: chemistry and technology*, 2nd ed., rev.Expanded. New York: M. Dekker, 1988.

[84] Y. Wen *et al.*, "A novel oligomer containing DOPO and ferrocene groups: Synthesis, characterization, and its application in fire retardant epoxy resin," *Polymer Degradation and Stability*, vol. 156, pp. 111–124, Oct. 2018, doi: 10.1016/j.polymdegradstab.2018.08.010.

[85] S. G. Prolongo, G. del Rosario, and A. Ureña, "Comparative study on the adhesive properties of different epoxy resins," *International Journal of Adhesion and Adhesives*, vol. 26, no. 3, pp. 125–132, Jun. 2006, doi: 10.1016/j.ijadhadh.2005.02.004.

[86] D. Hull, *An introduction to composite materials*. Cambridge ; New York: Cambridge University Press, 1981.

[87] M. Delucchi *et al.*, "A methodological approach for monitoring the curing process of fairing compounds based on epoxy resins," *Progress in Organic Coatings*, vol. 123, pp. 20–26, Oct. 2018, doi: 10.1016/j.porgcoat.2018.06.005.

[88] X. Ma *et al.*, "Synthesis of degradable hyperbranched epoxy resins with high tensile, elongation, modulus and low-temperature resistance," *Composites Part B: Engineering*, vol. 192, pp. 1–29, Jul. 2020, doi: 10.1016/j.compositesb.2020.108005.

[89] C. V. Opelt and L. A. F. Coelho, "On the pseudo-ductility of nanostructured epoxy resins," *Polymer Testing*, vol. 78, p. 105961, Sep. 2019, doi: 10.1016/j.polymertesting.2019.105961.

[90] D. Jackson dos Santos, J. R. Gouveia, M. Philipp, A. C. Augusto, N. M. Ito, and J. K. Krüger, "Temperature modulated optical refractometry: A novel and practical approach on curing and thermal transitions characterizations of epoxy resins," *Polymer Testing*, vol. 77, p. 105915, Aug. 2019, doi: 10.1016/j.polymertesting.2019.105915.

[91] C. Lou and X. Liu, "Functional dendritic curing agent for epoxy resin: Processing, mechanical performance and curing/toughening mechanism," *Composites Part B: Engineering*, vol. 136, pp. 20–27, Mar. 2018, doi: 10.1016/j.compositesb.2017.09.073.

[92] Q. Bao, B. Wang, Y. Liu, Q. Wang, and Z. Yang, "Epoxy resin flame retarded and toughed via flexible siloxane chain containing phosphaphenanthrene," *Polymer Degradation and Stability*, vol. 172, p. 109055, Feb. 2020, doi: 10.1016/j.polymdegradstab.2019.109055.

[93] H. Li, G. Chen, H. Su, D. Li, L. Sun, and J. Yang, "Effect of the stoichiometric ratio on the crosslinked network structure and cryogenic properties of epoxy resins cured at low temperature," *European Polymer Journal*, vol. 112, pp. 792–798, Mar. 2019, doi: 10.1016/j.eurpolymj.2018.10.051.

[94] M. Kisiel and B. Mossety-Leszczak, "Development in liquid crystalline epoxy resins and composites – A review," *European Polymer Journal*, vol. 124, p. 109507, Feb. 2020, doi: 10.1016/j.eurpolymj.2020.109507.

[95] F.-L. Jin, X. Li, and S.-J. Park, "Synthesis and application of epoxy resins: A review," *Journal of Industrial and Engineering Chemistry*, vol. 29, pp. 1–11, Sep. 2015, doi: 10.1016/j.jiec.2015.03.026.

[96] S. Morsch, Z. Kefallinou, Y. Liu, S. B. Lyon, and S. R. Gibbon, "Controlling the nanostructure of epoxy resins: Reaction selectivity and stoichiometry," *Polymer*, vol. 143, pp. 10–18, May 2018, doi: 10.1016/j.polymer.2018.03.065.

[97] F. C. Binks, G. Cavalli, M. Henningsen, B. J. Howlin, and I. Hamerton, “Investigating the mechanism through which ionic liquids initiate the polymerisation of epoxy resins,” *Polymer*, vol. 139, pp. 163–176, Mar. 2018, doi: 10.1016/j.polymer.2018.01.087.

[98] Y. Lu *et al.*, “Preparation of Epoxy Resins with Excellent Comprehensive Performance by Thiol-Epoxy Click Reaction,” *Progress in Organic Coatings*, vol. 139, p. 105436, Feb. 2020, doi: 10.1016/j.porgcoat.2019.105436.

[99] Z. Shen, Z. Xia, and Y. Zhang, “Characterization and properties of epoxy resin (E-20) modified with silicone intermediate RSN-6018,” *Progress in Organic Coatings*, vol. 114, pp. 115–122, Jan. 2018, doi: 10.1016/j.porgcoat.2017.10.014.

[100] D. Laouchedi, B. Bezzazi, and C. Aribi, “Elaboration and characterization of composite material based on epoxy resin and clay fillers,” *Journal of Applied Research and Technology*, vol. 15, no. 2, pp. 190–204, Apr. 2017, doi: 10.1016/j.jart.2017.01.005.

[101] G. Gibson, “Epoxy Resins,” in *Brydson’s Plastics Materials*, Elsevier, 2017, pp. 773–797.

[102] S. Zhou *et al.*, “Highly improving the mechanical and thermal properties of epoxy resin via blending with polyetherketone cardo,” *Composites Communications*, vol. 13, pp. 80–84, Jun. 2019, doi: 10.1016/j.coco.2019.03.003.

[103] B. Minisini, S. Rolère, J.-F. Coulon, and F. Poncin-Epaillard, “Influence of the chemical composition and formulation of fluorinated epoxy resin on its surface characteristics,” *European Polymer Journal*, vol. 112, pp. 452–460, Mar. 2019, doi: 10.1016/j.eurpolymj.2019.01.035.

[104] V. D. Ramos, H. M. da Costa, V. L. P. Soares, and R. S. V. Nascimento, “Modification of epoxy resin: a comparison of different types of elastomer,” *Polymer Testing*, vol. 24, no. 3, pp. 387–394, May 2005, doi: 10.1016/j.polymertesting.2004.09.010.

[105] S. Levchik, A. Piotrowski, E. Weil, and Q. Yao, “New developments in flame retardancy of epoxy resins,” *Polymer Degradation and Stability*, vol. 88, no. 1, pp. 57–62, Apr. 2005, doi: 10.1016/j.polymdegradstab.2004.02.019.

[106] H. Jiang *et al.*, “Novel biobased epoxy resin thermosets derived from eugenol and vanillin,” *Polymer Degradation and Stability*, vol. 160, pp. 45–52, Feb. 2019, doi: 10.1016/j.polymdegradstab.2018.12.007.

[107] I. K. Varma, V. B. Gupta, and N. K. Sini, “2.19 Thermosetting Resin – Properties,” in *Comprehensive Composite Materials II*, Elsevier, 2018, pp. 401–468.

[108] B. Ellis, Ed., *Chemistry and Technology of Epoxy Resins*. Dordrecht: Springer Netherlands, 1993.

[109] P. Jyotishkumar, N. Hameed, T. Kurian, and Y. Yu, Eds., *Nanocomposite materials: synthesis, properties and applications*. Boca Raton London New York: CRC Press, Taylor & Francis Group, 2017.

[110] C. Kanchanomai and A. Thammaruechuc, “Effects of stress ratio on fatigue crack growth of thermoset epoxy resin,” *Polymer Degradation and Stability*, vol. 94, no. 10, pp. 1772–1778, Oct. 2009, doi: 10.1016/j.polymdegradstab.2009.06.012.

[111] J. K. Fink, “Epoxy Resins,” in *Reactive Polymers Fundamentals and Applications*, Elsevier, 2013, pp. 95–153.

[112] J. Zhang, S. Chen, B. Qin, D. Zhang, P. Guo, and Q. He, “Preparation of hyperbranched polymeric ionic liquids for epoxy resin with simultaneous improvement of strength and toughness,” *Polymer*, vol. 164, pp. 154–162, Feb. 2019, doi: 10.1016/j.polymer.2019.01.003.

[113] F.-L. Jin and S.-J. Park, “Thermal properties of epoxy resin/filler hybrid composites,” *Polymer Degradation and Stability*, vol. 97, no. 11, pp. 2148–2153, Nov. 2012, doi: 10.1016/j.polymdegradstab.2012.08.015.

[114] H. Altenbach, J. Altenbach, and W. Kissing, “Classification of Composite Materials,” in *Mechanics of Composite Structural Elements*, Singapore: Springer Singapore, 2018, pp. 3–18.

[115] P. M. Ajayan, L. S. Schadler, and P. V. Braun, *Nanocomposite science and technology*. Weinheim: Wiley-VCH, 2003.

[116] J. C. J. Bart, *Additives in polymers: industrial analysis and applications*. Chichester, West Sussex, England ; Hoboken, NJ: John Wiley & Sons, 2005.

[117] K. D. Jansson, C. P. Zawodny, and T. P. Wampler, “Determination of polymer additives using analytical pyrolysis,” *Journal of Analytical and Applied Pyrolysis*, vol. 79, no. 1–2, pp. 353–361, May 2007, doi: 10.1016/j.jaap.2006.12.009.

[118] S. Al-Malaika, F. Axtell, R. Rothon, and M. Gilbert, “Additives for Plastics,” in *Brydson’s Plastics Materials*, Elsevier, 2017, pp. 127–168.

[119] V. Ambrogi, C. Carfagna, P. Cerruti, and V. Marturano, “Additives in Polymers,” in *Modification of Polymer Properties*, Elsevier, 2017, pp. 87–108.

[120] J. G. Drobny, “Additives,” in *Handbook of Thermoplastic Elastomers*, Elsevier, 2014, pp. 17–32.

[121] J. C. J. Bart, “Polymer additive analysis at the limits,” *Polymer Degradation and Stability*, vol. 82, no. 2, pp. 197–205, Jan. 2003, doi: 10.1016/S0141-3910(03)00196-4.

[122] E. A. Coleman, “Plastics Additives,” in *Applied Plastics Engineering Handbook*, Elsevier, 2017, pp. 489–500.

[123] S. A. Ashter, “Additives and Modifiers for Biopolymers,” in *Introduction to Bioplastics Engineering*, Elsevier, 2016, pp. 153–178.

[124] C. M. Hansen, “Polymer additives and solubility parameters,” *Progress in Organic Coatings*, vol. 51, no. 2, pp. 109–112, Nov. 2004, doi: 10.1016/j.porgcoat.2004.05.003.

[125] C. Kröhnke, “Polymer Additives,” in *Polymer Science: A Comprehensive Reference*, Elsevier, 2012, pp. 349–375.

[126] T. R. Crompton and Rapra Technology Limited, *Determination of additives in polymers and rubbers*. Shrewsbury, U.K.: Rapra Technology, 2007.

[127] C. Block, L. Wynants, M. Kelchtermans, R. De Boer, and F. Compernolle, “Identification of polymer additives by liquid chromatography–mass spectrometry,” *Polymer Degradation and Stability*, vol. 91, no. 12, pp. 3163–3173, Dec. 2006, doi: 10.1016/j.polymdegradstab.2006.07.015.

[128] A. Shrivastava, “Additives for Plastics,” in *Introduction to Plastics Engineering*, Elsevier, 2018, pp. 111–141.

[129] L. W. McKeen, “Additives,” in *Fluorinated Coatings and Finishes Handbook*, Elsevier, 2016, pp. 119–127.

[130] C. Reichardt and T. Welton, *Solvents and solvent effects in organic chemistry*, 4th, updated and enl. ed ed. Weinheim, Germany: Wiley-VCH, 2011.

[131] X.-F. Wu, Ed., *Solvents as reagents in organic synthesis: reactions and applications*, First edition. Weinheim: Wiley-VCH, 2017.

[132] C. Reichardt, *Solvents and solvent effects in organic chemistry*, 3rd, updated and enl. ed ed. Weinheim: Wiley-VCH, 2003.

[133] G. Wypych, Ed., *Use, health, and environment. Vol. 2: ...*, 2. ed. Toronto: ChemTec Publ, 2014.

[134] A. Babapoor, G. Karimi, and M. Khorram, “Fabrication and characterization of nanofiber-nanoparticle-composites with phase change materials by electrospinning,” *Applied Thermal Engineering*, vol. 99, pp. 1225–1235, Apr. 2016, doi: 10.1016/j.applthermaleng.2016.02.026.

[135] S. E. Jasim, M. A. Jusoh, M. Hafiz, and R. Jose, “Fabrication of Superconducting YBCO Nanoparticles by Electrospinning,” *Procedia Engineering*, vol. 148, pp. 243–248, 2016, doi: 10.1016/j.proeng.2016.06.595.

[136] Y. Wei *et al.*, “Fabrication of TiN/Carbon nanofibers by electrospinning and their electromagnetic wave absorption properties,” *Journal of Alloys and Compounds*, vol. 735, pp. 1488–1493, Feb. 2018, doi: 10.1016/j.jallcom.2017.11.295.

[137] X. Lu, L. Li, W. Zhang, and C. Wang, “Preparation and characterization of Ag_2S nanoparticles embedded in polymer fibre matrices by electrospinning,” *Nanotechnology*, vol. 16, no. 10, pp. 2233–2237, Oct. 2005, doi: 10.1088/0957-4484/16/10/043.

[138] V. V. Rodaev, A. O. Zhigachev, and Y. I. Golovin, “Fabrication and characterization of electrospun ZrO2/Al2O3 nanofibers,” *Ceramics International*, vol. 43, no. 17, pp. 16023–16026, Dec. 2017, doi: 10.1016/j.ceramint.2017.08.059.

[139] G.-X. Sun, F.-T. Liu, J.-Q. Bi, and C.-A. Wang, “Electrospun zirconia nanofibers and corresponding formation mechanism study,” *Journal of Alloys and Compounds*, vol. 649, pp. 788–792, Nov. 2015, doi: 10.1016/j.jallcom.2015.03.068.

[140] T. M. Alam, J. U. Otaigbe, D. Rhoades, G. P. Holland, B. R. Cherry, and P. G. Kotula, “Nanostructured polymer blends: Synthesis and structure,” *Polymer*, vol. 46, no. 26, pp. 12468–12479, Dec. 2005, doi: 10.1016/j.polymer.2005.10.079.

[141] D. Li *et al.*, “CuO nanostructures prepared by a chemical method,” *Journal of Crystal Growth*, vol. 282, no. 1–2, pp. 105–111, Aug. 2005, doi: 10.1016/j.jcrysgro.2005.04.090.

[142] T. Premkumar and K. E. Geckeler, “Palladium nanostructures: Solvent-less, one-pot mechano-chemical synthesis using poly(vinylpyrolidone) and catalytic activity,” *Colloids and Surfaces A: Physicochemical and Engineering Aspects*, vol. 456, pp. 49–54, Aug. 2014, doi: 10.1016/j.colsurfa.2014.05.006.

[143] X. Cheng, X. Zhang, H. Yin, A. Wang, and Y. Xu, “Modifier effects on chemical reduction synthesis of nanostructured copper,” *Applied Surface Science*, vol. 253, no. 5, pp. 2727–2732, Dec. 2006, doi: 10.1016/j.apsusc.2006.05.125.

[144] G. Xu, X. L. Wang, and G. Z. Liu, “Facile solvothermal synthesis of abnormal growth of one-dimensional ZnO nanostructures by ring-opening reaction of polyvinylpyrrolidone,” *Applied Surface Science*, vol. 329, pp. 137–142, Feb. 2015, doi: 10.1016/j.apsusc.2014.12.117.

[145] T. Tański, W. Matysiak, Ł. Krzemiński, P. Jarka, and K. Gołombek, “Optical properties of thin fibrous PVP/SiO2 composite mats prepared via the sol-gel and electrospinning methods,” *Applied Surface Science*, vol. 424, pp. 184–189, Dec. 2017, doi: 10.1016/j.apsusc.2017.02.258.

[146] L. Kumari, G. H. Du, W. Z. Li, R. S. Vennila, S. K. Saxena, and D. Z. Wang, “Synthesis, microstructure and optical characterization of zirconium oxide nanostructures,” *Ceramics International*, vol. 35, no. 6, pp. 2401–2408, Aug. 2009, doi: 10.1016/j.ceramint.2009.02.007.

[147] P. D. Gacia *et al.*, “Low-temperature synthesis of copper oxide (CuO) nanostructures with temperature-controlled morphological variations,” *Ceramics International*, vol. 41, no. 8, pp. 9426–9432, Sep. 2015, doi: 10.1016/j.ceramint.2015.03.323.

[148] M. Abushad, W. Khan, S. Naseem, S. Husain, M. Nadeem, and A. Ansari, “Influence of Mn doping on microstructure, optical, dielectric and magnetic properties of BiFeO3 nanoceramics synthesized via sol–gel method,” *Ceramics International*, vol. 45, no. 6, pp. 7437–7445, Apr. 2019, doi: 10.1016/j.ceramint.2019.01.035.

[149] A. Ali, S. Ambreen, R. Javed, S. Tabassum, I. ul Haq, and M. Zia, “ZnO nanostructure fabrication in different solvents transforms physio-chemical, biological and photodegradable properties,” *Materials Science and Engineering: C*, vol. 74, pp. 137–145, May 2017, doi: 10.1016/j.msec.2017.01.004.

[150] A. Haruna, I. Abdulkadir, and S. O. Idris, “Synthesis, characterization and photocatalytic properties of Bi0.85−XMXBa0.15FeO3 (M = Na and K, X = 0, 0.1) perovskite-like nanoparticles using the sol-gel method,” *Journal of King Saud University - Science*, p. S1018364719304732, May 2019, doi: 10.1016/j.jksus.2019.05.005.

[151] J. N. Hasnidawani, H. N. Azlina, H. Norita, N. N. Bonnia, S. Ratim, and E. S. Ali, “Synthesis of ZnO Nanostructures Using Sol-Gel Method,” *Procedia Chemistry*, vol. 19, pp. 211–216, 2016, doi: 10.1016/j.proche.2016.03.095.

[152] A. Lakshmanan *et al.*, “Effect of fuel content on nonlinear optical and antibacterial activities of Zn/Cu/Al2O4 nanoparticles prepared by microwave-assisted combustion method,” *Journal of King Saud University - Science*, p. S1018364719318415, Nov. 2019, doi: 10.1016/j.jksus.2019.11.031.

[153] H.-H. Sheu, S.-Y. Jian, T.-T. Lin, and Y.-W. Lee, “Effect of rotational speed of an electromagnetic stirrer on neodymium-doped yttrium aluminum garnet nanoparticle size during co-precipitation,” *Microelectronic Engineering*, vol. 176, pp. 33–39, May 2017, doi: 10.1016/j.mee.2017.01.020.

[154] L. Faxian, L. Jie, and C. Xueling, “Microwave-assisted Synthesis Silver Nanoparticles and Their Surface Enhancement Raman Scattering,” *Rare Metal Materials and Engineering*, vol. 46, no. 9, pp. 2395–2398, Sep. 2017, doi: 10.1016/S1875-5372(17)30204-7.

[155] M. Chandra, S. S. Indi, and P. K. Das, “First hyperpolarizabilities of unprotected and polymer protected copper nanoparticles prepared by laser ablation,” *Chemical Physics Letters*, vol. 422, no. 1–3, pp. 262–266, Apr. 2006, doi: 10.1016/j.cplett.2006.02.072.

[156] P. K. Baruah, A. K. Sharma, and A. Khare, “Effective control of particle size, surface plasmon resonance and stoichiometry of Cu@CuxO nanoparticles synthesized by laser ablation of Cu in distilled water,” *Optics & Laser Technology*, vol. 108, pp. 574–582, Dec. 2018, doi: 10.1016/j.optlastec.2018.07.044.

[157] S. Yang and J. Zhang, “Deposition of YBCO nanoparticles on graphene nanosheets by using matrix-assisted pulsed laser evaporation,” *Optics & Laser Technology*, vol. 109, pp. 465–469, Jan. 2019, doi: 10.1016/j.optlastec.2018.08.039.

[158] P. V. Kazakevich, A. V. Simakin, V. V. Voronov, and G. A. Shafeev, “Laser induced synthesis of nanoparticles in liquids,” *Applied Surface Science*, vol. 252, no. 13, pp. 4373–4380, Apr. 2006, doi: 10.1016/j.apsusc.2005.06.059.

[159] T. Tsuji, D.-H. Thang, Y. Okazaki, M. Nakanishi, Y. Tsuboi, and M. Tsuji, “Preparation of silver nanoparticles by laser ablation in polyvinylpyrrolidone solutions,” *Applied Surface Science*, vol. 254, no. 16, pp. 5224–5230, Jun. 2008, doi: 10.1016/j.apsusc.2008.02.048.

[160] M. A. Gondal, T. F. Qahtan, M. A. Dastageer, T. A. Saleh, Y. W. Maganda, and D. H. Anjum, “Effects of oxidizing medium on the composition, morphology and optical properties of copper oxide nanoparticles produced by pulsed laser ablation,” *Applied Surface Science*, vol. 286, pp. 149–155, Dec. 2013, doi: 10.1016/j.apsusc.2013.09.038.

[161] J. Yu, J. Nan, and H. Zeng, “Size control of nanoparticles by multiple-pulse laser ablation,” *Applied Surface Science*, vol. 402, pp. 330–335, Apr. 2017, doi: 10.1016/j.apsusc.2017.01.094.

[162] G. Takebe, T. Takagi, M. Suzuki, and M. Hiramatsu, “Preparation of polymeric nanoparticles of cyclosporin A using infrared pulsed laser,” *International Journal of Pharmaceutics*, vol. 414, no. 1–2, pp. 244–250, Jul. 2011, doi: 10.1016/j.ijpharm.2011.05.012.

[163] M. Saito, K. Yasukawa, T. Umeda, and Y. Aoi, “Copper nanoparticles fabricated by laser ablation in polysiloxane,” *Optical Materials*, vol. 30, no. 7, pp. 1201–1204, Mar. 2008, doi: 10.1016/j.optmat.2007.05.049.

[164] A. A. Menazea, “One-Pot Pulsed Laser Ablation route assisted copper oxide nanoparticles doped in PEO/PVP blend for the electrical conductivity enhancement,” *Journal of Materials Research and Technology*, p. S2238785419321313, Jan. 2020, doi: 10.1016/j.jmrt.2019.12.073.

[165] Zaydoon T. Mohammed Noori, Shehab A. Kadhim, Manal M. Abdullah, “Cu2O nanoparticles preparation by Pulse Laser Ablation in Liquid Phase method (PLALP),” *Iraqi Journal of Physics, 2019*, vol. Vol.17, no. No.42, p. PP. 141-146, 2019, doi: DOI: 10.20723/ijp.17.42.141-146.

[166] P. N. Barnes, P. T. Murray, T. Haugan, R. Rogow, and G. P. Perram, “In situ creation of nanoparticles from YBCO by pulsed laser deposition,” *Physica C: Superconductivity*, vol. 377, no. 4, pp. 578–584, Sep. 2002, doi: 10.1016/S0921-4534(02)00919-X.

[167] I. M. Budiati, F. Sa’adah, N. D. Rifani, and A. Khumaeni, “Effect of solvent in the synthesis of colloidal copper nanoparticles by pulse laser ablation method,” Surakarta, Indonesia, 2019, p. 020003, doi: 10.1063/1.5141616.

[168] J.-H. Rakebrandt, Y. Zheng, H. Besser, T. Scharnweber, H. J. Seifert, and W. Pfleging, “Laser-assisted surface processing for functionalization of polymers on micro- and nano-scale,” *Microsyst Technol*, Sep. 2019, doi: 10.1007/s00542-019-04633-7.

[169] R. Rawat, A. Tiwari, N. Arun, S. V. S. N. Rao, A. P. Pathak, and A. Tripathi, “Solvents Effect on the Morphology and Stability of Cu/CuO Nanoparticles Synthesized at High Fluence Laser Ablation,” *ChemistrySelect*, vol. 4, no. 35, pp. 10471–10482, Sep. 2019, doi: 10.1002/slct.201902344.

[170] A. Simakin, I. Baimler, O. Uvarov, I. Rud’, and V. Krasnoshekov, “Obtaining of nanoparticles of Sc, Ti, V, Cr, Mn, Fe, Co, Ni with controlled sizes and properties using laser ablation,” *IOP Conf. Ser.: Earth Environ. Sci.*, vol. 390, p. 012036, Nov. 2019, doi: 10.1088/1755-1315/390/1/012036.

[171] Iulia GRAUR, “Studiul proprietăţilor mecanice ale materialelor epoxidice aditivate cu substanţe ionice prin strategii de dispersie bazate pe utilizarea ultrasunetelor (teză de doctorat).” Universitatea „Dunărea de Jos” din Galaţi, 2015.

[172] Georgel Mihu, “Studiul proprietăţilor sistemelor epoxidice modificate cu solvenţi organici (teză de doctorat).” Universitatea „Dunărea de Jos” din Galaţi, 2016.

[173] T. Kavitha, T. Vasantha, P. Venkatesu, R. S. Rama Devi, and T. Hofman, “Thermophysical properties for the mixed solvents of N-methyl-2-pyrrolidone with some of the imidazolium-based ionic liquids,” *Journal of Molecular Liquids*, vol. 198, pp. 11–20, Oct. 2014, doi: 10.1016/j.molliq.2014.07.002.

[174] G. Engelhardt and H. Fleig, “1-Methyl-2-pyrrolidinone (NMP) does not induce structural and numerical chromosomal aberrations in vivo,” *Mutation Research/Genetic Toxicology*, vol. 298, no. 3, pp. 149–155, Jan. 1993, doi: 10.1016/0165-1218(93)90035-C.

[175] H. Wang, K. Xie, L. Wang, and Y. Han, “N-methyl-2-pyrrolidone as a solvent for the non-aqueous electrolyte of rechargeable Li-air batteries,” *Journal of Power Sources*, vol. 219, pp. 263–271, Dec. 2012, doi: 10.1016/j.jpowsour.2012.07.065.

[176] K. R. Reddy, D. B. K. Kumar, G. S. Rao, P. B. S. Sri, and C. Rambabu, “Vapor–liquid equilibria and excess molar volumes of N-methyl-2-pyrrolidone with 2-alkoxyethanols,” *Fluid Phase Equilibria*, vol. 336, pp. 52–58, Dec. 2012, doi: 10.1016/j.fluid.2012.08.030.

[177] P. Gnanakumari, P. Venkatesu, K. R. Mohan, M. V. P. Rao, and D. H. L. Prasad, “Excess volumes and excess enthalpies of N-methyl-2-pyrrolidone with branched alcohols,” *Fluid Phase Equilibria*, vol. 252, no. 1–2, pp. 137–142, Mar. 2007, doi: 10.1016/j.fluid.2006.12.012.

[178] H.-M. Li, S.-Y. Yang, J.-W. Wang, L.-S. Long, R.-B. Huang, and L.-S. Zheng, “Coordination steric effect of N,N-dimethylformamide, N,N-dimethylacetamide and N-methyl-2-pyrrolidone on the assembly of coordination polymers,” *Polyhedron*, vol. 29, no. 14, pp. 2851–2856, Sep. 2010, doi: 10.1016/j.poly.2010.07.007.

[179] C. Moreno-Marrodan, F. Liguori, and P. Barbaro, “Sustainable processes for the catalytic synthesis of safer chemical substitutes of N-methyl-2-pyrrolidone,” *Molecular Catalysis*, vol. 466, pp. 60–69, Apr. 2019, doi: 10.1016/j.mcat.2019.01.014.

[180] T. M. Letcher, J. Łachwa, and U. Domańska, “The excess molar enthalpies and volumes of (N-methyl-2-pyrrolidinone+an alkan-1-ol) at T=298.15K,” *The Journal of Chemical Thermodynamics*, vol. 34, no. 10, pp. 1581–1599, Oct. 2002, doi: 10.1016/S0021-9614(02)00202-1.

[181] C. Moreno-Marrodan, F. Liguori, and P. Barbaro, “Sustainable processes for the catalytic synthesis of safer chemical substitutes of N-methyl-2-pyrrolidone,” *Molecular Catalysis*, vol. 466, pp. 60–69, Apr. 2019, doi: 10.1016/j.mcat.2019.01.014.

[182] J. K. Fink, S. Thomas, and V. P. M., Eds., *Handbook of engineering and specialty thermoplastics*. Hoboken : Salem, Mass: Wiley ; Scrivener, 2010.

[183] R. Awasthi *et al.*, “Poly(vinylpyrrolidone),” in *Engineering of Biomaterials for Drug Delivery Systems*, Elsevier, 2018, pp. 255–272.

[184] V. K. Thakur and M. K. Thakur, *Handbook of polymers for pharmaceutical technologies. volume 3. volume 3.* 2015.

[185] P. A. Williams, Ed., *Handbook of industrial water soluble polymers*. Oxford ; Ames, Iowa: Blackwell Pub, 2007.

[186] J. Rodríguez-Hernández, *Polymers against Microorganisms*. Cham: Springer International Publishing, 2017.

[187] P. Molyneux, *Water-soluble synthetic polymers: properties and behaviour*. Boca Raton, Fla: CRC Press, 1984.

[188] B. V. Robinson, Ed., *PVP: a critical review of the kinetics and toxicology of polyvinylprrolidone (povidone)*. Chelsea, MI: Lewis Publishers, 1990.

[189] J. Njuguna, K. Pielichowski, and H. Zhu, Eds., *Health and environmental safety of nanomaterials: polymer nanocomposites and other materials containing nanoparticles*. Cambridge ; Waltham, MA: Woodhead Publishing, 2014.

[190] Y. Kourde-Hanafi *et al.*, "Influence of PVP content on degradation of PES/PVP membranes: Insights from characterization of membranes with controlled composition," *Journal of Membrane Science*, vol. 533, pp. 261–269, Jul. 2017, doi: 10.1016/j.memsci.2017.03.050.

[191] S. Zeng, Q. Su, and L.-Z. Zhang, "Molecular-level evaluation and manipulation of thermal conductivity, moisture diffusivity and hydrophobicity of a GO-PVP/PVDF composite membrane," *International Journal of Heat and Mass Transfer*, vol. 152, p. 119508, May 2020, doi: 10.1016/j.ijheatmasstransfer.2020.119508.

[192] T. D. Kusworo, W. Widayat, D. P. Utomo, Y. H. S. Pratama, and R. A. V. Arianti, "Performance evaluation of modified nanohybrid membrane polyethersulfone-nano ZnO (PES-nano ZnO) using three combination effect of PVP, irradiation of ultraviolet and thermal for biodiesel purification," *Renewable Energy*, vol. 148, pp. 935–945, Apr. 2020, doi: 10.1016/j.renene.2019.10.177.

[193] R. M. Lilleby Helberg, Z. Dai, L. Ansaloni, and L. Deng, "PVA/PVP blend polymer matrix for hosting carriers in facilitated transport membranes: Synergistic enhancement of CO2 separation performance," *Green Energy & Environment*, vol. 5, no. 1, pp. 59–68, Jan. 2020, doi: 10.1016/j.gee.2019.10.001.

[194] W.-Z. Lang, X. Zhang, J.-P. Shen, H.-P. Xu, Z.-L. Xu, and Y.-J. Guo, "The contrastive study of chemical treatment on the properties of PVDF/PFSA and PVDF/PVP ultrafiltration membranes," *Desalination*, vol. 341, pp. 72–82, May 2014, doi: 10.1016/j.desal.2014.02.027.

[195] Georgel Mihu, "Cercetări privind obținerea unor amestecuri cu polimeri termorigizi și termoplastici (cercetare postdoctorală)." Universitatea „Dunărea de Jos" din Galaţi, 2020.

[196] Radu Bosoancă, Vasile Bria, Claudiu Mereuță, Adrian Cîrciumaru, Iulian-Gabriel Bîrsan, "Tensile Analysis of Fabric Reinforced Materials." 2019, [Online]. Available: http:///www.revmaterialeplastice.ro.

[197] M. Dimofte, M. Bunea, A. Capatina, A. Cojan, R. Bosoanca, and A. Circiumaru, "Tensile and Bending Analysis of Fabric Reinforced Graded Epoxy Composites," *Mat.Plast.*, vol. 54, no. 2, pp. 362–367, Jun. 2017, doi: 10.37358/MP.17.2.4852.

[198] Ana Capatina, Vasile Bria, Marina Bunea, Iulian-Gabriel Birsan, "Tensile Behaviour of Fabric Reinforced Laminates and Plies," *Materiale Plastice (Mater. Plast.),* vol. Volume 56, no. Issue 2, pp. 370–377, Year 2019, doi: https://doi.org/10.37358/MP.19.2.5188.

[199] I. Bordeasu, A. Circiumaru, M. O. Popoviciu, I. Lazar, R. Badarau, and I. Groza, "Cavitation Erosion Behaviour on Thin Films of Polymer Blends Deposited Over Bronze Surfaces," *Mat.Plast.*, vol. 55, no. 3, pp. 286–290, Sep. 2018, doi: 10.37358/MP.18.3.5014.

[200] P.G. Zverev , T.T. Basiev , V.V. Osiko , A.M. Kulkov b, and V.N. Voitsekhovskii , V.E. Yakobson, "Physical, chemical and optical properties of barium nitrate Raman crystal," *Elsevier*, pp. 315–334, 1999.

[201] J. Wang *et al.*, "A highly structured hollow ZnO@Ag nanosphere SERS substrate for sensing traces of nitrate and nitrite species in pickled food," *Sensors and Actuators B: Chemical*, vol. 285, pp. 302–309, Apr. 2019, doi: 10.1016/j.snb.2019.01.052.

[202] J. L. Izquierdo, J. F. Montoya, A. Gómez, C. Paucar, and O. Morán, “Aspects of electronic transport in YBaCo4O7+δ pellets,” *Solid State Sciences*, vol. 12, no. 12, pp. 2073–2078, Dec. 2010, doi: 10.1016/j.solidstatesciences.2010.09.001.

[203] F. Zapata and C. García-Ruiz, “The discrimination of 72 nitrate, chlorate and perchlorate salts using IR and Raman spectroscopy,” *Spectrochimica Acta Part A: Molecular and Biomolecular Spectroscopy*, vol. 189, pp. 535–542, Jan. 2018, doi: 10.1016/j.saa.2017.08.058.